



Please cite the Published Version

Adams, Marcus J , Wadge, Matthew D , Sheppard, Drew, Stuart, Alastair and Grant, David M (2024) Review on onshore and offshore large-scale seasonal hydrogen storage for electricity generation: Focusing on improving compression, storage, and roundtrip efficiency. *International Journal of Hydrogen Energy*, 73. pp. 95-111. ISSN 0360-3199

DOI: <https://doi.org/10.1016/j.ijhydene.2024.05.421>

Publisher: Elsevier

Version: Published Version

Downloaded from: <https://e-space.mmu.ac.uk/635551/>

Usage rights:  [Creative Commons: Attribution 4.0](https://creativecommons.org/licenses/by/4.0/)

Additional Information: This is an open access article published in *International Journal of Hydrogen Energy*, by Elsevier.

Enquiries:

If you have questions about this document, contact openresearch@mmu.ac.uk. Please include the URL of the record in e-space. If you believe that your, or a third party's rights have been compromised through this document please see our Take Down policy (available from <https://www.mmu.ac.uk/library/using-the-library/policies-and-guidelines>)



Review on onshore and offshore large-scale seasonal hydrogen storage for electricity generation: Focusing on improving compression, storage, and roundtrip efficiency

Marcus J. Adams^{*}, Matthew D. Wadge, Drew Sheppard, Alastair Stuart, David M. Grant

Advanced Materials Research Group, Faculty of Engineering, University of Nottingham, University Park, Nottingham, NG7 2RD, United Kingdom

ARTICLE INFO

Handling Editor: Suleyman I. Allakhverdiev

Keywords:

Metal hydride buffer storage
Large-scale hydrogen storage
Metal hydride compression
Underwater hydrogen storage
Underground hydrogen storage
Oxyfuel process

ABSTRACT

This article presents a comprehensive review of the current landscape and prospects of large-scale hydrogen storage technologies, with a focus on both onshore and offshore applications, and flexibility. Highlighting the evolving technological advancements, it explores storage and compression techniques, identifying potential research directions and avenues for innovation. Underwater hydrogen storage and hybrid metal hydride compressed gas tanks have been identified for offshore buffer storage, as well as exploration of using metal hydride slurries to transport hydrogen to/from offshore wind farms, coupled with low pressure, high flexibility electrolyser banks. Additionally, it explores the role of metal hydride hydrogen compressors and the integration of oxyfuel processes to enhance roundtrip efficiency. With insights into cost-effectiveness, environmental and technology considerations, and geographical factors, this review offers insights for policymakers, researchers, and industry stakeholders aiming to advance the deployment of large-scale hydrogen storage systems in the transition towards sustainable energy.

1. Introduction

The evidence is clear that climate change due to greenhouse-driven global warming is significantly affecting many aspects of the economy, society, and the environment. 2023 has been confirmed to be the warmest on record, *ca.* 1.48 °C warmer than the long-term, pre-industrial average according to the EU's climate service [1]. This has accelerated the need to diversify from fossil fuels to more sustainable, abundant, green, and renewable fuel sources. Many countries are striving to achieve this through their net zero strategy, with hydrogen technology playing a necessary role. It is postulated that in the UK, H₂ can meet the net zero aims for all seven defined pathways, by achieving 100–591 TW h.year⁻¹ by 2050 [2].

To achieve the current levels of energy demand, one must consider the developments necessary to strengthen the pillars of the hydrogen economy. These are highlighted and discussed by various reviews in the literature and relate specifically to production [3–8], storage [3–17], transportation [3,4,6,15] and usage [4–8,17,18]. Additional areas of importance include techno-economics [4,6,9,10,15–17], systems integration [4,9,15–17], and practical aspects of implementation (such as

legislation, safety, purification etc.) [7,8,10,15,18]. The recurring conclusions about the barriers to implementing the hydrogen economy are centred around cost, efficiency, technology durability and, in particular, storage.

Storage is critically important, especially to achieving the scale necessary to deliver energy demands. At each point along the chain from production, through transport and distribution and ultimately final usage, appropriate storage at scale should be addressed. The feasibility and success of large-scale green hydrogen storage are influenced by market dynamics, policy support, and regulatory frameworks [19], meaning large scale storage could be technologically feasible, but hampered by regulatory and/or policy shortfalls. Despite this, overcoming the technological barrier is still a significant challenge, particularly in achieving production and storage at scale.

A key driver for Large-scale Hydrogen Storage (LSHS) is dependent on ideal locations for hydrogen production. For example, Scotland has the potential to produce industrial-scale H₂ quantities from onshore and offshore wind, with the European North Sea region potentially increasing grid development in both Europe and the North Sea by up to 50% [20]. A key benefit of utilising offshore wind is the wind speed at

^{*} Corresponding author.

E-mail addresses: marcus.adams1@nottingham.ac.uk (M.J. Adams), Matthew.Wadge3@nottingham.ac.uk (M.D. Wadge), Drew.Sheppard@nottingham.ac.uk (D. Sheppard), Alastair.Stuart@nottingham.ac.uk (A. Stuart), David.Grant@nottingham.ac.uk (D.M. Grant).

<https://doi.org/10.1016/j.ijhydene.2024.05.421>

Received 31 March 2024; Received in revised form 18 May 2024; Accepted 27 May 2024

Available online 7 June 2024

0360-3199/Crown Copyright © 2024 Published by Elsevier Ltd on behalf of Hydrogen Energy Publications LLC. This is an open access article under the CC BY license (<http://creativecommons.org/licenses/by/4.0/>).

sea is much higher (7–10 m s⁻¹), and more consistent, allowing generation of significantly higher power than that produced by a land-based wind turbines [21–23]. This is due to natural, land-based wind barriers, such as hills, mountain ranges, forests, and cities, which can reduce speeds by up to 40% [24]. Megastructures, such as floating wind turbines, which may be more than 30 km off the coast, are exposed to waves and a saline environment that accelerates corrosion. Additionally, their location away from the coast and without displaced personnel requires very high reliability of operations. Travel times in case of failure or emergency are increased and downtime periods consequently rise with the economic impact that this implies. A recent review has identified that suitable offshore locations with high wind capacity factors can enable competitive green hydrogen production, however the main barrier to implementation is the economics [25]. The subsequent transport of hydrogen at sea would be via pipelines or ships, and on land, pipeline, or trucks. We briefly review the status on this in section 2.

The recent UK Large Electricity Storage report has underscored the necessity for long-term storage solutions spanning years, if not decades, a feat only achievable in most countries through large-scale hydrogen storage (LSHS) [26]. While numerous reviews examine existing technologies that could be implemented within LSHS, light attention, to the best of the authors' knowledge, has been given to strategies for enhancing LSHS beyond current best practices, whether implemented onshore, offshore, or a combination of both.

This paper explores the avenues for improving the efficiency of LSHS, which currently stands at ca. 40% round-trip efficiency (lower heating value (LHV)) [26]. The round-trip efficiency (RTE) for energy storage refers to the ratio between the energy supplied to the storage system and the energy retrieved from it. Specifically, we investigate the feasibility of enhancing this efficiency through the integration of thermal compression and oxyfuel processes. Furthermore, given the versatility of LSHS in accommodating both onshore and offshore hydrogen production and storage, this review also examines the literature and explores methods to enhance buffer storage and again, the potential utilisation of thermal compression, utilising waste heat from electrolyzers, not only for efficiency gains, but improvements in flexibility. By presenting these findings, this review aims to seed future research directions for LSHS, offering critical insights and perspectives from the authors to drive

advancements in the field.

2. Transporting hydrogen

The International Energy Agency (IEA) has highlighted hydrogen as an increasingly important piece of the net zero emissions by 2050 puzzle [27]. To achieve this, green hydrogen production must increase substantially, as well as determining effective methods to transport energy around the world. A growing domain for hydrogen production is within offshore wind generation. A question that requires answering is whether hydrogen should be generated onshore or offshore, or some optimal combination of the two. As such, this section focuses heavily on pipeline transmission, with a brief discussion on other methods, namely liquid hydrogen, ammonia, and liquid hydrogen organic carriers, which are not explicitly linked to LSHS for electricity generation, but rather a downstream application. Fig. 1 summarises key aspects on each option covered in this article. Adsorbents such as activated carbon and metal organic frameworks are not discussed due to the low operating temperatures (around liquid nitrogen) [28].

2.1. Pipeline transmission: compressed gas

Hydrogen transportation utilises various methods including pipelines, compressed gas tanks, liquefied hydrogen tankers, ammonia, or liquid organic hydrogen carriers. According to an IEA report, for distances up to 1500 km, piping hydrogen is the most cost-effective option when including all the supply chain stages (conversion, transmission, distribution, storage, and reconversion). Beyond this distance, shipping via ammonia or liquid organic hydrogen carriers becomes more economical [29]. A Guidehouse report echoes this sentiment, highlighting that repurposed pipelines are notably more cost-efficient than new installations, and the cost per kilogram of hydrogen decreases with larger pipe diameters [30]. Newly built and moderately worn pipelines are considered as candidates for repurposing, where it is highly desirable to sufficiently clean the pipeline before re-commissioning. Cleaned pipelines have reduced energy loss due to a reduction in pipe roughness and the fact that cleaned pipes have removed chemicals that can react with hydrogen [31]. Natural gas transmission typically contains small

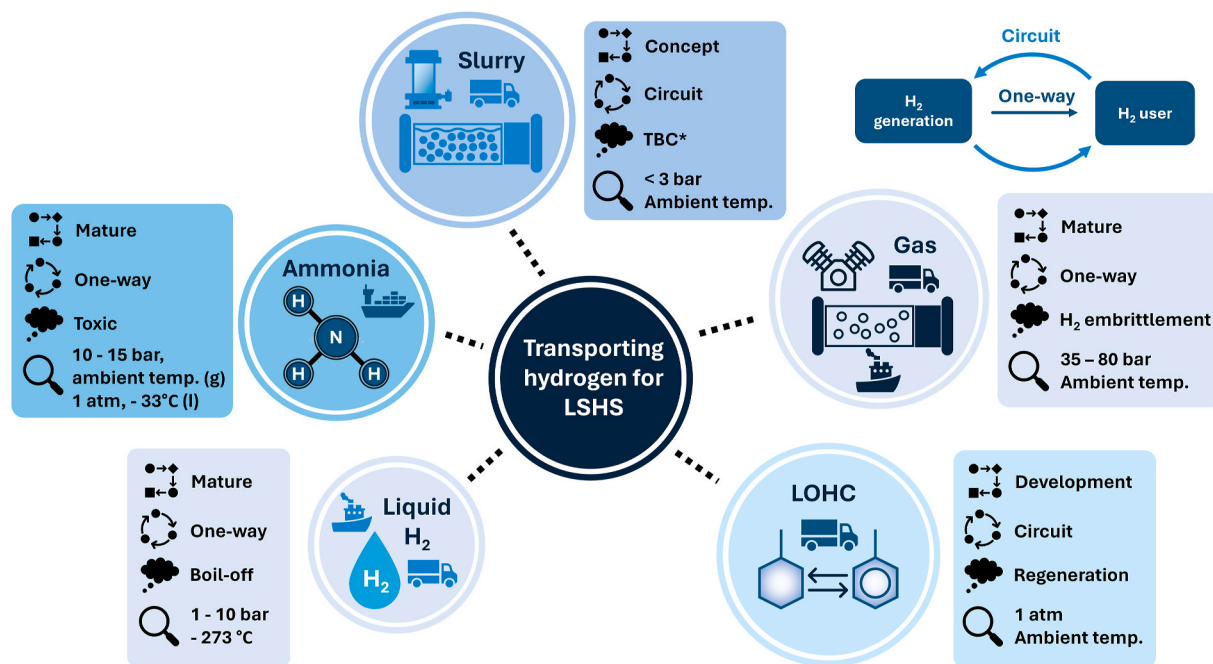


Fig. 1. Infographic summarising methods to transport hydrogen around that is linked to large-scale hydrogen storage, either integral to the process or indirectly. The summary categories are i) maturity of technology, ii) operation, iii) one key consideration, iv) typical transport conditions. *TBC = to be confirmed.

amounts of sulphur compounds that can deposit onto the pipe inner wall, flow restrictors, compressor inlets, filter housing outlets and valves [32]. Reaction with hydrogen to form hydrogen sulphide is known to accelerate hydrogen embrittlement [33], as such it is critical to remove such impurities for pipe longevity.

For large-scale hydrogen storage, fabrication of pipeline infrastructure can draw upon decades of experience. Current practices in oil refineries and chemical plants operate hydrogen piping between 35 and 80 bar [34]. While the maximum pressure in hydrogen gas transmission pipelines usually caps at 210 bar [35], projects like the Zero Regio Project have demonstrated feasibility at higher pressures, supplying refuelling stations with 1000 bar pipelines over short distances using DIN 1.4462 stainless steel [34].

A case study from China explored optimal pressure depending on distance and annual transmission quantity, revealing that at 1000 km, the optimal pressure ranges from 40 bar for <0.5 Mtons/year, to 80 bar for 2 Mtons/year [36]. Materials selected for hydrogen containment must exhibit strong resistance to hydrogen embrittlement. Typically, transmission and distribution pipelines employ low-strength carbon steels at room temperature, while austenitic stainless steels are common in local gas distributors like manifolds. Although carbon steels are cost-effective, at present those intended for hydrogen service undergo special processing to ensure uniform, fine-grained microstructures [33].

For both onshore (buried) and offshore (on seabed) transmission, internal, external, and cathodic protection is employed to protect from environmental conditions. An example approach is an API 5 L grade X52 steel pipe, with internal coating of Al–Zn alloy (Galvalume®), and an external coating of epoxy, adhesive and polyolefin [31,37]. Then, sacrificial anodes can be added to the hull of the line pipe for additional protection [31]. Composite pipelines are also possible, one such example is the Soluforce H2T pipe, where an inner liner of high-density polyethylene (HDPE) is bonded with aluminium as a hydrogen permeation barrier, with the liner reinforced with fibre reinforced plastics (FRP), and finally covered with HDPE as a protective layer. The FRP is itself reinforced with aramid fibre [38]. Operating conditions up to 42 bar and 65 °C and 50 year shelf-life are possible [38].

2.2. Pipeline transmission: metal hydride slurry

A potential option not commonly explored is hydrogen pipeline transport using metal hydride slurries. Despite the extensive research on metal hydride hydrogen storage, the literature on slurries is notably sparse in comparison, with a review provided in Ref. [39]. While the majority of studies concentrate on inert fluids like silicone oil, it is noteworthy that flammable fluids tested demonstrated superior hydrogen permeation rates [39]. Notably, a mixture of 40–50 wt % hydride in fluid has been identified for effective cycling [40]. Kinetic experiments of $\text{LaNi}_{4.8}\text{Al}_{0.2}$ (AB_5) suspended in cyclohexane and ethanol found the rate limiting steps to be the dissolution of hydrogen in the solvent and reaction of hydrogen with the metal alloy [41]. The reaction rate of metal hydride slurries is also a function of pressure and mass transfer. With effective mixing, conversion of LaNi_5 to hydride achieved 90%+ conversion in 1 min or less – demonstrating viability [42]. In addition, MgH_2 based slurries were shown to stay in suspension for months and are easily stirred back into suspension, if the particles settle [43]. As an example material, $\text{LaNi}_{4.91}\text{Al}_{0.09}$ can achieve 90% H_2 capacity at < 2 bar [44].

This approach offers several advantages, including enhanced safety by shielding the hydride from exposure to air [45], simplified design of metal hydride reactors, and the potential for operating at lower transmission pressures. In the context of offshore wind farms, employing flexible electrolysis would mitigate curtailment. Strategies such as modular electrolyzers can foster adaptability, particularly if they operate at low pressures (<3 bar), facilitating quicker transition from shut-down to operation, and longer shelf-life. Hydride slurries show potential here as by blending hydrogen into a low-pressure hydride slurry, it

becomes feasible to store hydrogen directly from electrolysis at low pressure and transport it to shore using rugged slurry pumps. This eliminates the need for compression, streamlining the offshore process and reducing maintenance and service expenses. Upon reaching shore, releasing the hydrogen will necessitate low-grade heat. If the slurry is being pumped to an industrial process, it is likely low-grade heat would be available. Globally, it is estimated up to 50% of the global primary energy consumption is wasted/lost as low grade heat [46]. A disadvantage of this concept is that the slurry must be pumped back in a circuit to replenish spent slurry. A counter to this could be the lower cost of the slurry low pressure pipelines. Although steel/concrete pipes are common (with the option of abrasion-resistant lining), non-ferrous pipes are also widespread, such as high-density polyethylene (HDPE) within the mining or wastewater industries [47]. HDPE is durable and resistant to abrasion, flexible, chemically resistant, and inexpensive [47], and a candidate for low pressure hydrogen gas transmission [48]. To fully gauge the suitability of this concept however, further work would be required on suitable metal hydride/fluid materials, testing against pipeline material(s), material composition, levelized costs and technical experiments.

2.3. Liquid hydrogen

Liquid H_2 is candidate for H_2 transport and storage due to its high density of 71 kg m^{-3} at 20 K and 1 atm. It is an established technology; however, its disadvantages are high energy usage, extensive insulation requirements, boil-off management, and capital costs. Review on liquid hydrogen plant technology can be found here [9,49,50].

Using liquid H_2 necessitates a process plant, therefore labour and maintenance considerations are required. Due to this, liquid H_2 will be produced on dedicated islands or near to shore. A recent article discusses the advantages and disadvantages of hydrogen use as a maritime fuel and the major hurdles that come with the storage of hydrogen on board ships [51]. For example, the Suiso Frontier, a prototype liquid hydrogen carrier ship, designed by Kawasaki Heavy Industries, is designed to carry, and distribute liquified hydrogen from Australia to Japan [52]. The LCOS for liquid hydrogen was calculated as 4.57 USD/kg with a possible future of 0.95 USD/kg [53].

2.4. Ammonia

Ammonia is of interest in energy storage, as a zero-carbon fuel and as a hydrogen carrier [54]. A key benefit is its established infrastructure for production, storage, and distribution. Ammonia can be directly combusted in engines, although due its poor combustion characteristics (high auto-ignition temperature, low flammability, and low flame speed), fuel blending is usually adopted, typically with hydrogen. For example, an addition of 10 % hydrogen in supercharged conditions improved the efficiency by 37% and maximum power by 59 % [54]. Storage is a mature technology, with large volume storage possible as a liquid above 9 bar at 20 °C, or at atmospheric pressure and – 33 °C [55]. As a hydrogen carrier, it has a high hydrogen content of 17.8 wt% H_2 , and a volumetric energy density of 15.6 MJ/L, higher than compressed hydrogen (5.6 MJ/L at 700 bar) and liquid hydrogen (8.5 MJ/L) [55].

The IEA Ammonia Technology Roadmap outlines the future trajectory of ammonia production and its diverse applications [56]. Presently, global consumption is around 200 million tons per year (Mt NH_3/y), with 70% allocated to fertilisers and the remainder to industrial sectors like plastics. Projecting ammonia as an energy carrier, the roadmap envisages two scenarios for 2050: the Sustainable Development Scenario (SDS) and the Net Zero Emissions Scenario (NZE). The SDS entails a demand of 410 Mt NH_3/y , while the NZE ambitiously requires 550 Mt NH_3/y , earmarking significant portions for shipping and power generation. Meeting this demand underscores a pivotal challenge in realising ammonia's potential as an energy carrier. Given the maturity of the Haber-Bosch process, directing resources towards electrifying it emerges

as a pragmatic approach. A study investigated retrofitting a 1000 t NH_3/d plant, replacing steam methane reforming with electrolysis while retaining steam-driven turbines. The analysis revealed a plant efficiency of 51% [57], notably behind current best practice steam methane reforming (at 63% [58]). The key energy loss in green Haber-Bosch is the H_2 production. In section 4, we mention the potential for metal hydride hydrogen compressors (MHHCs) to utilise electrolyser waste heat for LSHS. It is possible that MHHCs could be applied to Haber-Bosch as well.

Another proposed approach is to push the Haber-Bosch process towards low pressure (and temperature) ammonia synthesis, away from the traditional 100–150 bar reactors. Doing so will allow greater flexibility in production processes, due to faster shutdown to operation periods. To do this, however, will require breakthroughs in low pressure ammonia catalysis, and replacement of the traditional NH_3 condensation route with metal chlorides absorbents, enabling high agility and lower energy losses [58]. Another issue with low pressure ammonia synthesis is the catalysts involved. High pressure reactors use inexpensive iron pellets, while low pressure reactors tend to be ruthenium based on oxides supports, or even hydrides [59]. A replacement for ruthenium would be advantageous, potentially through alloy-based nitrides such as a commonly explored nitride of $\text{Co}_3\text{Mo}_3\text{N}$ [59].

Realising ammonia's potential as a versatile hydrogen carrier and next-generation fuel also requires focus on the decomposition reaction. Industrially, ammonia crackers use nickel supported on an alumina catalyst, and operate between 850 and 950 °C, with advantages of heat resistance and mechanical longevity [60]. The decomposition strategies may differ depending on the application. For example, it would be advantageous if on-board ammonia combustion could involve hydrogen generation through utilising engine waste heat, whereas ceramic kiln furnaces could generate the required heat to adopt current industry practices using Ni- Al_2O_3 catalysts. Both ammonia synthesis and decomposition would benefit from step change catalyst advancements.

Due to the toxicity of ammonia, it is generally assumed unsuitable for small scale transportation, but has been earmarked for the shipping industry. The BloombergNEF Hydrogen Economy Outlook report states a benchmark levelized cost of storage (LCOS) at 2.83 USD/kg, with a future projection of 0.9 USD/kg [53]. A recent study proposed suitable production, import and export locations for the ammonia shipping industry, detailing large production zones in coastal areas in west Africa, Middle East, northwest Australia, west North America and west South America (Chile) [61]. Australia has potential to be the most dominant green ammonia exporter, accounting for 50% of the global export [61]. Currently, however it ranks 19th in ammonia production globally [61], illustrating large production challenges (and opportunity). The total investment is estimated to be USD 2 trillion [61]. As H_2 is feedstock for NH_3 production, this article provides a good benchmark for nearby large-scale H_2 production zones and scoping large-scale H_2 storage zones.

2.5. Liquid organic hydrogen carriers

Liquid Organic Hydrogen Carriers (LOHCs) are a class of chemical compounds that can reversibly store and release hydrogen through chemical reactions [62]. An example leading candidate LOHC is dibenzyl toluene/Perhydro-dibenzyl toluene that exhibits 6.2 wt% H_2 and 57 kg $\text{H}_2 \text{ m}^{-3}$ [62]. Dibenzyl toluene is a common major component in Marlotherm SH, a widely used thermal oil and has a competitive price of 65 EUR/kg H_2 [62]. Another candidate is toluene, a common solvent at only 5 EUR/kg H_2 [62].

In general, a key challenge is to find cheaper dehydrogenation catalysts that exhibit high activity, selectivity, and long service life. Usually, expensive noble metals are employed, such as Pd, Pt, Ru, and Rh. While Ni and Mo have been extensively researched as alternatives, they often fall short in terms of reactivity, operational temperature range, and service life [63]. For dibenzyl toluene, full hydrogenation at 150 °C

and 50 bar using a Ru/ Al_2O_3 catalyst was demonstrated, and 97% conversion for dehydrogenation using Pd/C catalyst at 310 °C was achieved [64].

LOHCs have been explored for H_2 transportation, with applications ranging from inter-city to inter-continental transport. Estimated costs range from 0.96 to 3.87 USD/kg for inter-city transport and 3.87 to 6.70 USD/kg for inter-continental journeys [53]. Again, in the context of onshore/offshore large-scale hydrogen storage, LOHCs may be produced on a dedicated island or close to shore for direct export to industry via land in trucks or pipelines. Much like metal hydride slurries, if LOHCs were adopted for pipelines transmission or trucks, a return journey is necessary. However, LOHCs also have a large energy requirement, where the enthalpy of reaction for Dibenzyl toluene and toluene are -65.4 kJ/mol H_2 and -66.3 kJ/mol H_2 respectively [62].

2.6. Electrolyser location: onshore or offshore

Many papers and reports have studied comparisons between hydrogen pipeline transmission and electrical cables [31,65–68]. In general, the problem is complex, and the answer, like any model/forecast, heavily depends on the assumptions. H_2 pipelines offer several advantages. These include reduced infrastructure costs compared to laying electrical cables, reduced transmission losses for gas in pipelines and potential repurposing of existing infrastructure, and a smoother environmental approval process for gas pipelines compared to high voltage cables [68]. For comparison, the energy loss in a new 48" (1.22 m) pipeline at 80 bar reference pressure was calculated at 1.7 % loss/1000 km [31] (another source 0.5–1 % loss/1000 km [65]), while a high voltage direct current (HVDC) cable is 3.5 % loss/1000 km and a high voltage alternating current (HVAC) cable is 6.7 % loss/1000 km [67].

A DNV report examined three offshore wind cases, HVAC, HVDC and offshore electrolysis with pipeline transport. The report stated there is a transition zone between 100 and 150 km, where the levelized cost of hydrogen (LCOH) is cheaper to move energy through hydrogen pipelines than HVDC cables. The LCOH represents the average cost of producing 1 kg of hydrogen over the entire lifetime of the hydrogen production system, where it considers both the initial investment costs and the operational costs associated with hydrogen production. At distances less than 100 km, the cheapest LCOH is through HVAC cables. Also, hydrogen pipelines have greater scalability, as hydrogen pipelines can be combined to form a backbone grid to transport hydrogen from several windfarms [66]. Further, HVDC lines can transfer up to 12 GW, while H_2 pipelines can transfer 20–30 GW [65]. Conversely, electrical cables provide operators with increased flexibility, allowing for the option of selling electricity or producing hydrogen based on economic viability. However, viewing these technologies and projects in isolation is counterproductive. Instead, they should be seen as complementary elements, each offering unique benefits [68].

In the case of LSHS, hydrogen generation is required, so the necessary H_2 generation losses are incurred either onshore or at sea. As H_2 transmission losses are lower than HVDC cables, it is logical that H_2 is generated as close to the energy source as possible. However, more in-depth case-by-case analysis is required that includes aspects such as pumping stations, consideration of flexibility (batteries/ H_2 buffer) and with accompanying space and maintenance, and even if there is desire to utilise the oxygen, which would favour onshore electrolysis (see section 4.2).

3. Onshore and offshore large-scale hydrogen storage options

3.1. Large-scale options

3.1.1. Underground hydrogen storage

Underground hydrogen storage is recognised as the only economically viable method to store hydrogen at the TWh scale, with salt caverns

considered the most attractive option [26]. Reviews and reports on these technologies, specifically salt caverns, depleted gas fields, aquifers, and lined rock caverns can be found elsewhere [69–73]. These reviews and reports cover technical aspects, challenges, economic analysis, and current projects. A BloombergNEF report stated the possible future levelized cost of storage (LCOS) at the highest reasonable cycling rate to be 0.11 USD/kg, 1.07 USD/kg and 0.23 USD/kg for salt caverns, depleted gas fields and rock caverns, respectively [53].

UK researchers have recently recognised that years of hydrogen storage will be necessary, where the East Yorkshire basin is an excellent location for onshore salt caverns [74]. The cost of a 300 000 m³ salt cavern in the East Yorkshire basin (containing 122 GW h [LHV]) equated to a projected salt cavern construction cost of 7 GBP/kg H₂ at a maximum cavern pressure of 270 bar [75]. Once including additional costs, including geological surveys, pipelines, topside and above ground facility, land, owners, contingency and cushion gas cost, the total cost was 93 GBP/kg H₂ [75]. An offshore salt cavern was costed, based in the East Irish Sea equating to 32 GBP/kg H₂ for the salt cavern construction cost, and 487 GBP/kg H₂ for the total cost [75]. It was also found that many of the formations in the Irish Sea basin are unsuitable for salt caverns, except the Preesall Halite Formation [76]. However, the higher offshore salt caverns cost was due to the construction of the 4-legged tower ‘jacket’ structure and topside facility, equalling 63 % of the total investment cost [75]. It is logical that construction of offshore salt caverns will incur similar costs, and therefore onshore salt caverns would be the preferred option, if possible. The construction of salt caverns involves the disposal of brine [69], necessitating careful consideration of its environmental impact. While salt produced from this process is released into the sea at a controlled rate [77], the scenario where large amounts of brine from a significant expansion in salt caverns, within a condensed timeframe has not yet been analysed. To the best of the author’s knowledge, there hasn’t been a comprehensive Life Cycle Assessment (LCA) conducted on this matter, though a similar evaluation has been undertaken regarding brine disposal in desalination plants [78].

Regarding Northern Europe, there is significant offshore and onshore (<50 km to coast) salt cavern capacity, with the UK, Germany and Denmark containing significant capacity [66,79]. Conveniently, salt

cavern and depleted gas fields are located close to existing and planned wind farms, as shown in Fig. 2.

Hydrogen salt caverns exist today, but no hydrogen storage facilities in depleted gas fields are present. A study examined using the Rough Gas Storage Facility (a depleted gas field in the UK) for H₂ storage instead of natural gas, which concluded a cushion gas ratio of 45–55 %, 50–100 bar delivery pressures, and a 120-day withdrawal period. Operating as a H₂ store, it could deliver 40 % of the daily energy compared to natural gas. No intractable technical barriers were identified, with clay-bearing sandstone and iron oxides stable under reservoir conditions, leakage losses of 0.035 % after 12 months and less than 3.7 % H₂ loss through biological activity, in which purification treatment might be needed for H₂S formation [80].

The development of a depleted gas field into storage typically spans a duration of 3–10 years [71], and up to 5 years to complete a salt cavern [69]. A recent report highlighted the UK’s necessity for 30+ TWh of storage [26], where if this demand were hypothetically met by hydrogen stored in salt caverns, it would entail the creation of ca. 250 salt caverns, each with a capacity of 300 000 m³. With 2050 looming just 26 years from now, this simple analysis indicates the global imperative to move forward with underground energy storage, considering the long construction timeframes.

3.2. Buffer storage options

Buffer stores are units that ensure a steady flow of hydrogen to the compressor. They are positioned after electrolysis and before compression, where the store provides a buffer for the compressor when the electrolyser output varies due to renewable energy fluctuations.

3.2.1. Compressed gas pressure vessels

If the outlet electrolyser pressures are 35 bar, and inlet compressor pressures are 20 bar, then standard compressed gas vessels will exhibit low useable volumetric density. For instance, if a buffer store operates between a charging pressure of 35 bar and a discharging pressure of 20 bar, the useable density is 1.2 kg m⁻³. Wind output can change significantly [26]; thus, the buffer store requirement may be large. Onshore plants may have the required land for large stores, but then the cost of

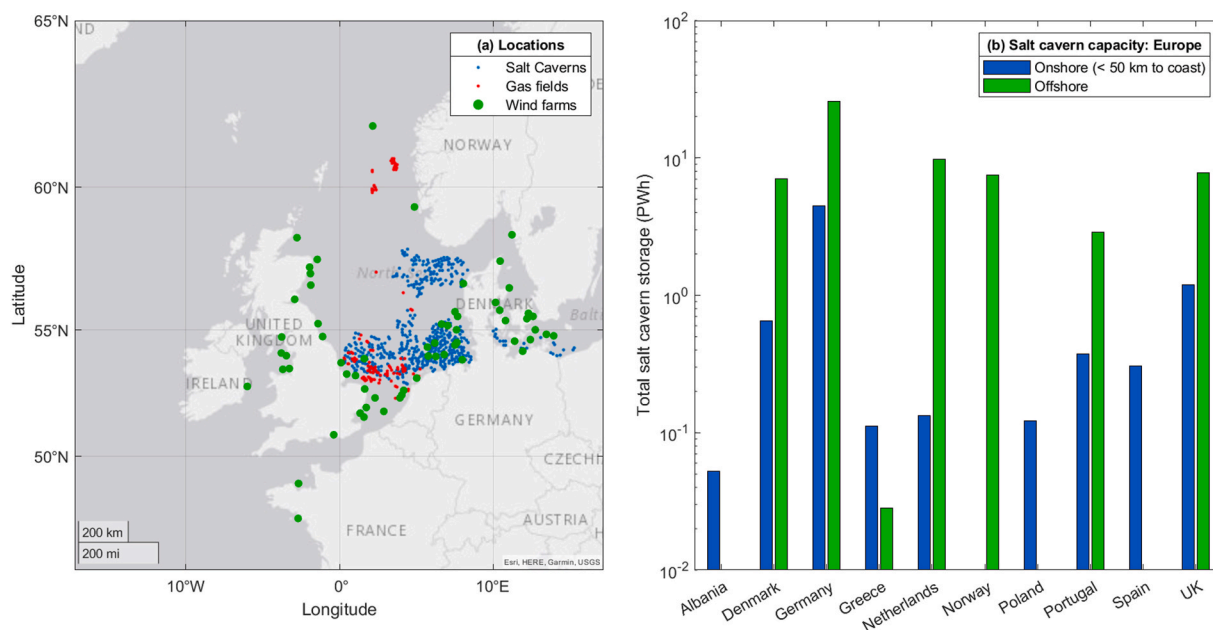


Fig. 2. (a) Approximate locations of offshore salt caverns [79], prominent gas field locations (extracted from Ref. [81]), and wind farm locations (extracted from Ref. [82]) primarily in the North Sea. (c) Technical potential for close to shore and offshore salt caverns in Europe (extracted from Ref. [79]).

material will become an important factor, whereas for offshore wind facilities, the space available is constrained, so application for more compact buffer stores is desirable. Larger vessels are spherical containment, whereas small to medium size are cylindrical with semi-elliptical ends. The criteria when selecting the type of pressure vessel shape ultimately considers strength, cost, and ease of production, where the balance tips in favour of spherical vessels at large capacity. In the future, machine learning and artificial intelligence techniques may be useful for optimising the type, size and shape of compressed gas storage vessels [83,84].

3.2.2. Metal hydrides

However, with potentially large supply fluctuations, a more compact buffer store solution is desirable, in which metal hydrides (MHs) could provide a solution. MHs offer much larger volumetric densities compared to compressed gas, especially for buffer stores. Therefore, a small inclusion of metal hydride can support a large increase in buffer functionality. MHs are hydrogen bonded to metals and are an extensively researched technology for hydrogen storage [85–87]. The following generic metal hydride reaction is,



where M is a metal/alloy and MH_x is a metal hydride. Hydrogenation is exothermic, whereas dehydrogenation is endothermic. The equilibrium pressure (P_{eq}) of the hydrogen bound to metal and in the gaseous state is a function of temperature through the van't Hoff equation (eq. (2)), where $P_0 = 1$ bar, R is the universal gas constant, T is temperature and ΔS^0 and ΔH^0 are the entropy and enthalpy of formation respectively.

$$\ln\left(\frac{P_{eq}}{P_0}\right) = -\frac{\Delta S^0}{R} + \frac{\Delta H^0}{RT} \quad 2$$

With nano-sized particles the surface energy becomes an important factor, and assuming a sphere, the van't Hoff equation can be modified to,

$$\ln\left(\frac{P_{eq}}{P_0}\right) = -\frac{\Delta S^0}{R} + \frac{\Delta H^0 + (3V_M\Delta_{M \rightarrow MH_2}/r)}{RT} \quad 3$$

where V_M is the molar volume of the metal, r is the radius of a spherical particle and $\Delta_{M \rightarrow MH_2}$ is the surface term [88]. Another source of enthalpy reduction can be from strain at the grain boundary [88].

Within the framework of a hybrid compressed gas metal hydride buffer store, equilibrium pressure plays a pivotal role. During standard operation, the hydride remains in a charged state, at high pressure. However, when the supply diminishes, the pressure within the buffer store begins to decline. Once the gas pressure descends below the equilibrium pressure threshold, dehydrating initiates, raising pressure and serving as a buffer for the downstream unit.

The selection criteria for these materials depends on the operating conditions, cost, availability of material, ease/safety of manufacture and handling, and performance (reaction kinetics, H_2 storage density and weight). Examples of ambient temperature metal hydrides are AB, AB₅, AB₂, and V-based BCC alloys. An example of an AB hydride is TiFe_{0.85}Mn_{0.15} [89], AB₅ examples include LaNi_{4.91}Al_{0.09} and LaNi_{4.8}C_{0.02} [44], example AB₂ materials are multi-component, such as Ti_{0.65}Zr_{0.35}(Cr,Mn,Fe,Ni)₂ [90] and a V-based BCC alloy example is Ti₅₂V₁₂Cr₃₆ [91]. Regarding MH buffer stores, hydride materials ideally require:

- A 'flat' plateau to maximise the stored hydrogen in the MH (see Fig. 7b for illustration),
- minimal hysteresis to maximise stored hydrogen in the MH (see Fig. 7b for illustration),
- fast reaction kinetics to handle the fast response required.

Considering the above metal hydrides, V-based BCC alloys are in early-stage research and do not readily operate between the required pressure range of 20–35 bar at ambient temperature, the AB₂ class of hydrides are significantly cheaper than AB₅ hydrides based on rare-earth elements and their intrinsic hydrogen diffusion kinetics can be five orders of magnitude times faster than AB-based hydrides, such as TiFeH_x [92,93]. As such, due to these factors and the desire for tunability (so can be deployed globally depending on the local conditions), potential suitable metal hydrides materials considered here for buffer stores are AB₂ intermetallic alloys. Developments in machine learning and artificial intelligence may be useful in this regard for both identifying promising metal hydride materials [94,95] and aiding in metal hydride reactor design [96,97].

AB₂ alloys are materials where A contains elements that occupy the A-site (e.g. Ti, Zr, Mg, rare earths), while the B contains element that occupy the B-site (e.g. Fe, Ni, Mn, Cr, V, Co, Al) [87]. Incorporating a fraction of the buffer tank volume using MH can significantly increase useable density from 1.2 to 6.3 kg m⁻³ at 10 vol% MH and up to 13.9 kg m⁻³ at 25 vol% MH, if possible. (see Fig. 3). The calculations are based on assuming 1 wt% useable H₂ (between 35 and 20 bar), and a crystal metal hydride density of 5200 kg m⁻³. This value was derived based on the crystal density of Ti_{1.2}Mn_{1.8}, of 6365 kg m⁻³ [98], and assuming a 25% volume expansion upon hydriding [87].

Metal hydride hydrogen storage, excluding buffer storage, is more cost-effective for flexible megawatt-hour (MWh) scale applications rather than the terawatt-hour (TWh) scale required for large-scale hydrogen storage (LSHS). Although AB type metal hydride hydrogen storage has been proven effective for MWh scale uses [99], it does not meet the TWh scale demands necessary for LSHS. Therefore, this article focuses on how metal hydrides can be utilised to improve the process and flexibility for TWh scale applications.

3.2.2.1. Metal hydride tank considerations. The utilisation of metal hydride reactions necessitates heat supply for dehydrogenation and heat removal during hydrogenation, due to their endothermic and exothermic reactions, respectively. Achieving this poses challenges due to the poor heat transfer characteristics of metal hydride powders, leading to a deceleration of the reaction rate. Consequently, reactor and tank designs employ intricate heat transfer architectures to mitigate this limitation. These designs often incorporate various elements such as tubing, fins, aluminium foam, and additive manufacturing [100–104]. The compaction of powders into pellets or plates, supplemented with graphite, is common to improve thermal conductivity and packing density to improve heat transfer and volumetric density [105,106]. Fig. 4 illustrates such strategies employed by researchers.

However, a MH buffer store allows for an alternative design approach compared to conventional methods. Through the compaction of hydrides into pellets or plates, and the concurrent use of hydrogen as both the heat transfer fluid and reactant, a relatively simple to install and scalable design is possible [107]. This is largely due to the substantial flow rate of hydrogen passing through the buffer store, facilitating efficient convective heat transfer, while the fluid properties of hydrogen and medium size pellets facilitate a low-pressure drop and short conductive heat transfer distance.

For MH offshore/onshore H₂ storage, the operating conditions are the environment temperature and outlet electrolyser pressures. AB₂ materials are an ideal candidate here, where the cost of AB₂ materials (including manufacture) are currently commercially available varying between 1000 and 2000 GBP/kg H₂, depending on compositions, H₂ capacity, and tonnage. These materials exhibit high H₂ density of ≈40–50 kg m⁻³ (after accounting for powder packing density and total system volume) and are heavy at 1–2 wt% H₂ (system) [108]. For comparison, a study exploring the levelized cost of hydrogen storage for metal hydrides predicted a CAPEX of 1120 GBP/kg H₂ based on a 1USD:0.8GBP exchange rate [109]. For stationary offshore/onshore H₂

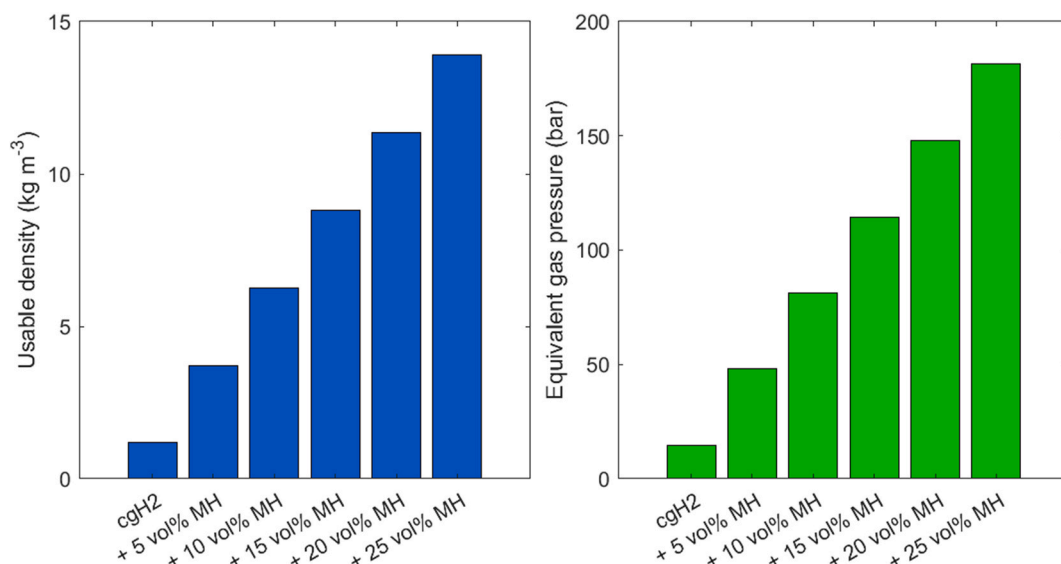


Fig. 3. Advantage of partial metal hydride inclusion in a H₂ buffer store operating between 35 and 20 bar considering (a) the useable density of the buffer store, and (b) the ‘equivalent gas density’ at respective vol% metal hydride.

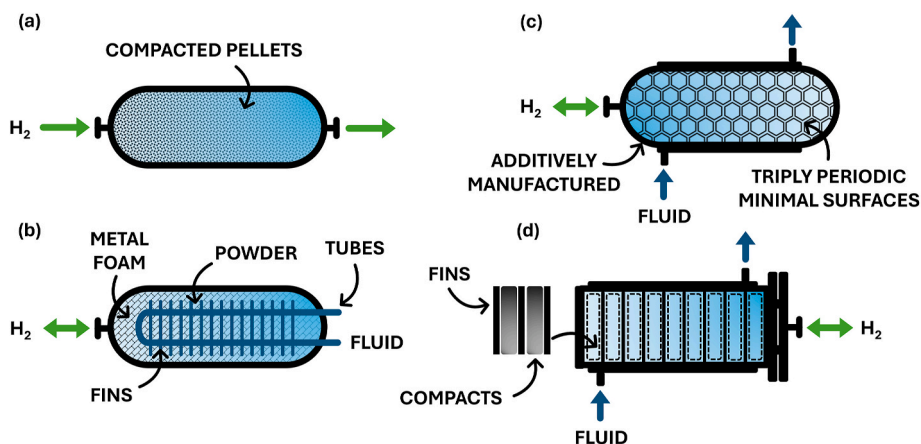


Fig. 4. Infographic describing metal hydride tank design based on (a) using hydrogen as both a heat transfer fluid and reactant, (b) metal foam, fins, and tubes in a powdered bed, (c) a unibody additive manufactured tank using triply periodic minimal surfaces, and (d) metal hydride compacts between fins. It is common to have a mixture of the strategies listed above.

buffer storage, weight becomes less critical while factors like cost, durability, maintenance frequency, and hydrogen storage density take precedence.

Considering suitability between offshore/onshore, the maintenance and operability of the metal hydride material is minimal, so there is no preference if the MH tanks are offshore/onshore. AB₂ materials (such as Ti_{0.98}Zr_{0.02}V_{0.43}Fe_{0.09}Cr_{0.05}Mn_{1.5}) have maintained performance up to 42 000 cycles if the purity of hydrogen gas is maintained [110]. It is mostly likely the peripheral units will need maintenance first (valves etc) on harsh offshore conditions. To improve resilience from impurities (such as O₂ and H₂O), hydrides can be doped with fluorine or mixed with polymers [111–114].

3.2.3. Underwater hydrogen storage

Underwater hydrogen storage follows similar principles to underwater compressed air storage. With underwater storage, the hydrostatic pressure from water depth is utilised, where internal and hydrostatic pressures are roughly equal, minimising containment needs. The storage operates under isobaric conditions, enhancing energy density without needing cushion gas [115]. An advantage of underwater hydrogen storage is the lightweight structures enable tethering not directly on the

ocean seabed, reducing the effect on the marine environment.

The hydrostatic pressure increases by 1 bar for every 10 m in depth [115]. Due to the size limit of underwater storage, they may find use as additional buffer storage before H₂ compression (see Fig. 6) in deep-water offshore wind facilities. The Hydrostor project explored underwater compressed air energy storage and determined that suitable depths were greater than 200 m, but ideally 400 m [116]. As offshore wind platforms can be deliberately positioned at depths >300 m, underwater hydrogen storage is therefore a compelling possibility for buffer storage.

3.2.3.1. Underwater flexible walled storage. Underwater storage in flexible fabric walls, known as ‘energy bags’, were originally developed for compressed air energy storage [115,117]. A working 5 m diameter prototype positioned 25 m offshore in Orkney, Scotland was tested for 3 months. The energy bags showed air leakage of <1.2 % per day, where the leaks concentrated around the stitching/seams [115]. This would be more problematic with H₂ due to it being a small molecule, however a large amount of the leaking was attributed to installation and scratching/tearing of the wall, which could be reduced with more durable materials. A simple diagram of an energy bag and attachment to a

floating wind platform is shown in Fig. 6a and d.

A study exploring the optimum shape considering non-zero pressure, non-zero circumferential stress and hanging ballast, resulted in a cost of 907 GBP/MWh storing 2249 m³ of air at 50.96 bar (or 11 356 GBP per bag) with a radius of ca. 8 m [117]. Converting to GBP/kg H₂ at 50 bar (500 m) and 5 °C, is 1.20 GBP/kg H₂ (9508 kg H₂) for the cost of materials only. At 4 bar (40 m depth), the cost is 14.50 GBP/kg H₂ (782 kg H₂). These costs would increase with installation and design extras (ballast, reinforcement, support structures, flexible tubing, control systems, labour etc). The total lifetime and maintenance cost also requires further research.

NASA undertook tests in the 1980s to capture liquid hydrogen boil off with metal hydrides, where NASA used hydrogen released from large balloons to simulate low-pressure high-flow rate liquid hydrogen boil-off. Hydrogen stored in balloons was sent into a hydride. It was found that the hydride was being poisoned to different amounts based on the balloon material (see Fig. 5). Potential reasons included residual air in the balloon due to insufficient purging, oxygen and/or water vapour permeation through the skin of the balloon and leaching of compounds from the balloon material by the hydrogen. As such, this is a potential issue that requires more clarification if this technology is to be introduced. Table 1 outlines the hydrogen permeation coefficients for other potential elastomers with chloro-isobutene-isoprene rubber (CIIR) the lowest. The NASA report using silicone vacuum grease in addition to an elastomer is an interesting strategy as it is evident it dramatically reduced cyclic capacity loss in the metal hydride compared to bare natural rubber.

3.2.3.2. *Underwater fixed walled storage.* Also proposed for compressed air systems, are underwater fixed walled storage [119,120]. Here, isobaric conditions are maintained by allowing seawater displacement, where Fig. 6c shows a simple diagram of underwater fixed wall storage based on a cylinder. As with air, hydrogen will diffuse into seawater (according to Henry's Law - the amount of dissolved gas in a liquid is directly proportional to its partial pressure above the liquid [121]), so must be considered. A potential solution to reduce diffusion is a movable non-permeable interface between H₂ and H₂O. Elastomer materials in Table 1 can be explored here. Again, the materials do not need to be structurally strong from a pressure perspective, but rather withstand seawater conditions and ocean currents, resistance to biological effects, and exhibit low hydrogen permeation rates. Similar to transporting low-pressure hydrogen in high density polyethylene (HDPE), the fixed

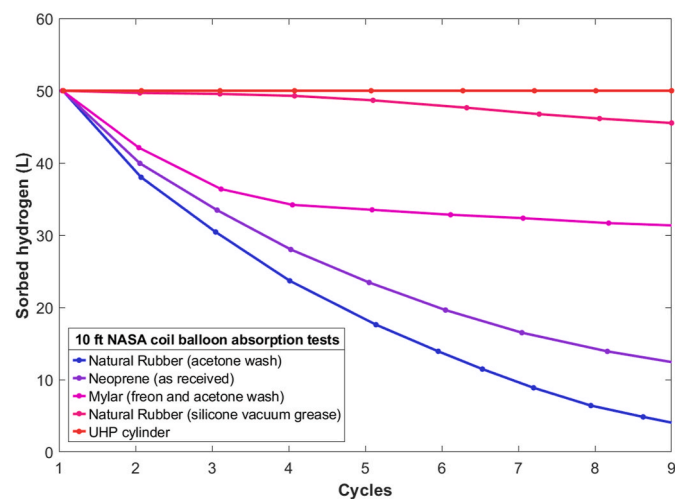


Fig. 5. Effect of hydrogen stored in various elastomers compared to an ultra-high purity (UHP) cylinder on cyclic sorption capacity of hydride. Hydrides adsorb the impurities, so it indicates better wall materials. Graph reproduced from NASA report [118].

wall material could be HDPE also (Table 1).

3.3. Other options

3.3.1. Underwater energy storage

3.3.1.1. *Ocean renewable energy storage.* The Ocean Renewable Energy Storage (ORES) concept utilises concrete spheres for energy storage positioned deep underwater, coupled with floating wind turbines. The principle is based on pumped-hydro storage plants. These spheres, tethered to the seabed, serve a dual function as both energy storage units and mooring structures [124,125]. During excess electricity production, water is pumped out of the sphere to store energy, and then allowed to flow back through a turbine to generate electricity and hydrogen, when needed. An illustration is shown in Fig. 6b. As such, the stored energy enables the electrolyser and compressor station to operate closer to steady state, but a disadvantage is the concrete spheres are directly placed on the seabed, affecting marine life. The ORES concept predicted viability between 200 and 700 m [124]. A similar project, the StEnSea concept (Stored Energy in the Sea), tested concrete spheres in Lake Constance, Europe [126]. The specific investment costs were 430–541 EUR/kWh (465–586 USD/kWh) [127].

3.3.1.2. *Buoyancy energy storage.* Buoyancy energy storage technology (BEST) uses an electric motor/generator for storing energy by descending a compressed gas unit underwater, and then generating electricity by allowing the unit to rise, where more energy is stored with greater depth. It is aimed at weekly energy storage with a cost projection of 50–300 USD/kWh using hydrogen between 10000 and 2000 m depth respectively [128]. It would serve a similar purpose to the ORES concept by smoothing transient responses for the electrolyser/compressor. Potential offshore locations are the Japanese and Chilean coast, however operating and maintaining this technology at such depths would be a challenge.

4. Improving the roundtrip efficiency and compression

To improve the large-scale hydrogen storage process, it is advantageous to enhance the roundtrip efficiency. For both onshore and offshore settings, a highly efficient process, and a low levelized cost is desirable. Whereas, with offshore scenarios, a very high reliability of operations is also necessary. Typically, traditional mechanical compression stands out as the prevalent technique for hydrogen compression. However, in offshore applications, numerous moving components such as pistons, coupled with exposure to saline environments and challenging accessibility to platforms, can pose maintenance challenges.

A comprehensive review on current technologies of hydrogen compression based on mechanical, cryogenic, electrochemical, adsorption and metal hydride compressors (MHHCs) has been discussed previously [129–131]. Of the compressors examined, MHHCs pose an interesting avenue, due to the reduced number of moving parts and the fact they are driven thermally.

4.1. Thermal hydrogen compression

A comprehensive review on MHHCs, including thermodynamics, materials between –50 and 240 °C and pressures from 0 to 4000 atm, and prototype compressors designs are detailed here [132]. This section will briefly cover MHHCs and discuss the potential and challenges of MHHCs specific to LSHS scenarios.

4.1.1. Metal hydride compressors thermodynamics

An examination of the thermodynamics of MHHCs has been conducted previously [133]. However, the existing literature on this subject appears to be limited, with certain aspects that may warrant further

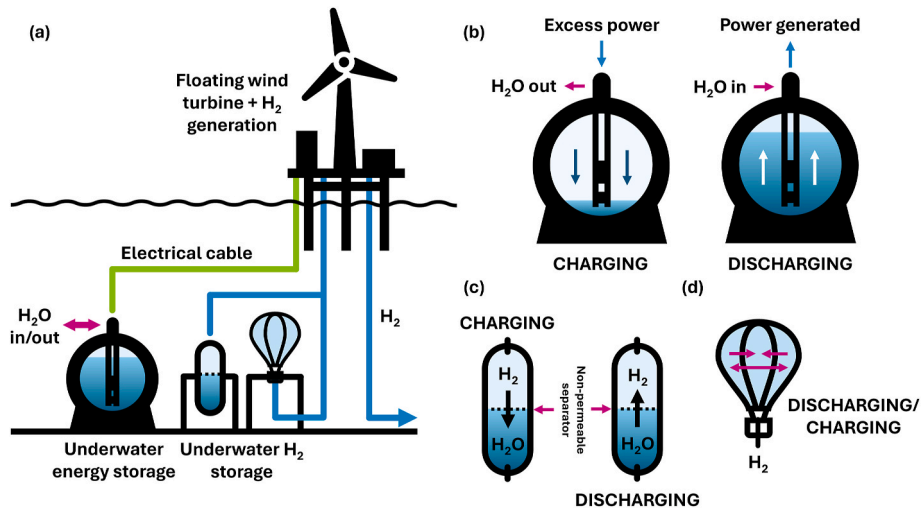


Fig. 6. (a) Potential underwater energy/hydrogen storage options when coupled with an offshore wind platform (b) Visualisation of underwater pumped water charge/discharge (c) Visualisation of underwater H₂ storage charge/discharge for isobaric cylinders and energy bags.

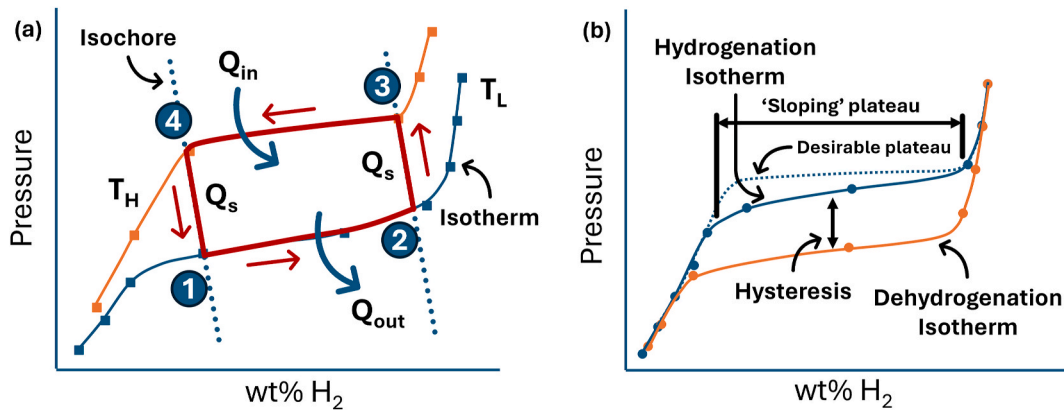


Fig. 7. (a) Illustration of the MHHC cycle on the isotherms at T_L and T_H . The isotherms are of alloy 4 in Table 2, $Ti_{30}V_{15.8}Mn_{49.4}(Zr_{0.5}Cr_{1.1}Fe_{2.9})$ between 20 °C (sorption) and 60 °C (desorption). Isochoric sensible heating/cooling is shown to illustrate the cycle. (b) The same system at 45 °C illustrating the ‘sloping’ plateau and hysteresis of the isotherms.

analysis and validation. Present literature uses a polytropic process during the sensible heating/cooling region [132], where the polytropic process is defined as $(pV^n = \text{constant})$ and depends on the polytropic index (n). To illustrate the cycle, $n = +\infty$ is assumed, giving an isochoric step – hence a Stirling cycle (an isochoric process is constant volume process). At present, the “best case” cycle of an AB_2 MHHC is shown in Fig. 7 and described below:

- 1–2: Isothermal compression (hydrogenation)
 - o Literature currently states that for an ideal material, where the progression $P_1 = P_2$, this step is also isobaric (a constant pressure process) [132,133].
 - o Gaseous hydrogen reacts with the metal. Progression from gas phase to being squeezed into the metal compresses the gas.
- 2–3: Sensible heating from T_L to T_H .
 - o The change in pressure is related to the van’t Hoff equation (eq. 2). This is an exponential relationship whereas the gas law is a straight proportion between P and T .
- 3–4: Isothermal expansion (dehydrogenation)
 - o Literature currently states that an ideal material has no hysteresis and the progression P_3 to P_4 is also isobaric [132,133].
 - o Hydrogen is released from the hydride. The gas is expanded as it escapes from the hydride.
- 4–1: Sensible cooling from T_H to T_L .

- o The change in pressure is related to the van’t Hoff equation (eq. 2)
- o Literature currently states an additional isobaric cooling of the hydrogen from T_H to T_L , while a polytropic cooling of the MH [132,133].

During step 1–2, heat is removed (Q_{out}) based on ΔH , and for 3–4, heat is input (Q_{in}) also based on ΔH . Steps 2–3 and 4–1 are sensible heating/cooling steps (Q_s) and heat can be regenerated here to improve cycle efficiency. Based on present literature, it would be advantageous for further in-depth analysis regarding steps 2–3 and 4 - 1. Note, the isochore in Fig. 7 will be a vertical line for an infinitely small dead space, and a horizontal line for an infinitely large dead space. Fig. 7 illustrates a small dead space volume that one would aim towards.

The Carnot efficiency (η_C) details the upper limit efficiency of any classical thermodynamic engine during conversion of heat into work [132].

$$\eta_C = 1 - \frac{T_L}{T_H} \tag{4}$$

The efficiency of MHHCs has also been investigated and shown in eq. (2), where Q is the heat of formation of MH, K_V is the dead space coefficient, σ is the heat recovery coefficient (regeneration), c_k is the heat capacity of MH container and bed, k_m is the coefficient accounting the mass ratio of the MH and the metalware, ψ is the mass fraction of

Table 1

Polymer options for underwater hydrogen storage. Permeability coefficients for plastics and elastomers (mol H₂ 10⁻⁹/(m s MPa)).

Description (Plastics)	Permeability coefficients at Temp. (K)				Ref.
	293	298	300	308	
High density polyethylene (HDPE)	0.60				[48]
Fiberspar - High density polyethylene (HDPE)	1.00				[122]
Ticona Forton - Polyphenylene sulphide (PPS)	0.70				[122]
Poly(vinyl chloride) (PVC) (unplasticised)	0.58		0.8		[123]
Poly(vinyl fluoride) (PVF)					0.18 [123]
Poly(vinyl fluoride) (PVF) (Kynar)					0.18 [123]
Description (Elastomers)	Permeability coefficients at Temp. (K)				Ref.
	293	298	308	353	
Chloro-isobutene-isoprene rubber (CIIR) (shore 70)	0.86				11.6 [123]
Acrylonitrile-butadiene rubber (NBR) (shore 70)	1.45				12.1 [123]
Acrylonitrile-butadiene rubber (NBR) (shore 60)	1.67				21.1 [123]
Chloro-sulfonyl-polyethylene (CSM) (shore 70)	1.31				9.28 [123]
Type of fluoro-rubber (FKM) (shore 70)	1.51				18.6 [123]

hydrogen in MH, ΔT are the temperature gradients in the heat supply (T_H side) and removal (T_L), and ΔT is the related to the temperature hysteresis in the sorption process [132,133].

$$\eta_{MHC} = \frac{Q(1 - K_V) \left(\eta_C - \left(\frac{\Delta T_H}{T_H} + \frac{\Delta T_L}{T_L + \Delta T_L} \right) \right)}{Q(1 - K_V) + (1 - \sigma) \left(c_k \frac{1-k_m}{\psi} (T_H - \Delta T_H + \Delta T_H^r - T_L + \Delta T_L - \Delta T_L^r) + Qk_V \right)}$$

5

MHHC performance efficiency (relative Carnot) (η_p) is shown in eq. (3).

$$\eta_p = \frac{Real}{Ideal} = \frac{\eta_{MHC}}{\eta_C} \quad 6$$

4.1.2. Applications of metal hydride compressors

The advantages of MHHCs for large-scale hydrogen storage are that electrolyser waste heat can be used to compress hydrogen [134], and excess waste heat can be thermally stored, enabling flexibility to the compressor unit. The waste heat is used to drive the dehydrogenation (endothermic) expansion side (3–4) in Fig. 7. For a typical first stage MH compressor material (see Table 2), the maximum enthalpy is 25 kJ mol H₂⁻¹ or 3.4 kW h kg H₂⁻¹, which is required to drive the expansion (dehydrogenation) “stroke”. If η_p is assumed as 60 % (5.6 kW h kg H₂⁻¹), then it is suitable to have a single MHHC to suitable pipeline transmission pressure. There is potential to have two MHHCs using electrolyser waste heat (based on an electrolyser system requirement of 54 kW h/kg H₂ and a balance of plant of 6 kW h/kg H₂ [135] (so 48 kW h/kg H₂ stack electrical input and a maximum waste heat of 8.6 kW h/kg H₂ from the higher heating value (HHV)), but it will require very high MHHC performance efficiencies (up to 80 %) and high electrolyser waste heat utilisation (high efficiency heat exchange of 90%). With two MHHCs, it is possible to reach up to 500+ bar from 30 bar with a second stage MHHC of enthalpy 20 kJ mol H₂⁻¹ (2.8 kW h/kg H₂) based on materials listed in Ref. [132]. This has potential to unlock areas that require high pressure storage, need high pressure green hydrogen for an industrial

process (such as ammonia synthesis), or enable additional options when moving hydrogen around. From a large-scale hydrogen storage perspective, MHHCs should be positioned with the electrolyser unit. As illustrated in Fig. 8, specifically addressing offshore wind and hydrogen production, the MHHC serves as the initial compressor station, followed by onshore mechanical compression for storage or industrial utilisation. Additionally, the setup incorporates potential MH and underwater hydrogen buffer storage for further versatility.

A bonus of MHHCs is that suitable materials are available in the literature. Table 2 covers AB₂ type alloys only, and intentionally does not include AB, AB₅ and V-based BCC alloys, of which examples of these alloys can be found here [132]. Only AB₂ materials are included for two reasons: 1) the tunability and 2) they can be (predominantly) rare-earth free.

These materials are Ti-based AB₂ alloys, enable compression of hydrogen from ca. 30–100 bar between ambient and electrolyser temperatures in a first stage MHHC. Places such as the North Sea will benefit due to colder ambient temperatures, enabling higher compression ratios.

4.1.3. Challenges of metal hydride compressors

Although first stage compressor AB₂ materials are well established and suitable for prototypes, further optimisation is necessary regarding cost and functionality. AB₂ materials cover a broad range of pressures and are even suitable for the 2nd stage compressor, examples are TiCrMn [136], TiCrMn_{0.7}Fe_{0.2}V_{0.1} [137], and TiCr_{1.5}Mn_{0.25}Fe_{0.25} [138]. From a technical material challenge perspective, suitable MHHC materials require [132]:

- (1) A large compression ratio regarding P_1 , P_2 , P_3 and P_4 between T_L to T_H (Fig. 7) based on the isotherm profiles.
- (2) A high useable wt.% H₂ to reduce material, which holds good cyclability.
- (3) Fast kinetics when progressing between 1–2 and 3–4 (in Fig. 7).
- (4) Small gradient between $P_1 \rightarrow P_2$ and $P_3 \rightarrow P_4$.
- (5) Small hysteresis, $\ln(P_S^m / P_D^m)$.

To aid material optimisation, a thermodynamic model has been developed for alloy selection of multi-stage MHHCs [139]. The other challenge with MHHCs for offshore and onshore large-scale hydrogen storage are engineering based and are outlined below.

- (1) Improving low performance efficiency (η_p).

To achieve high performance efficiency (η_p), it is necessary to achieve a low dead space volume, high working fluid (hydrogen) regeneration between stages 2–3 and 4–1, high cycle rate to reduce metal used (thereby reducing the sensible heat/cooling on the metal) - and/or heat recovery of the metal, and efficient heat transfer between source/sink to the metal hydride (stages 1–2 and 3–4), whereby the heat input/removed is transferred to drive the respective reaction, ideally, with minimal loss to the surroundings and minimal heat leakage to other components. Few examples in the literature utilise heat regeneration and exhibit rather low efficiencies, although a prototype by Ergenics Inc claimed a η_p of 69 % [132]. For utilisation in large-scale hydrogen storage and effective use of electrolyser waste heat, performance

Table 2

Potential suitable intermetallic alloys (or starting composition for refinement) for first stage MHCs based on using electrolyser waste heat. The ratio, $\ln(P_s/P_d)$, is the hysteresis between sorption and desorption PCIs, lower the better. (#) Calculated equilibrium pressures at stated ΔH_D and ΔS_D (assumed midpoint) between operating temperatures of 15–80 °C.

No.	Alloy	ΔS_D [J mol H ₂ ⁻¹ K ⁻¹]	ΔH_D [kJ mol H ₂ ⁻¹]	$P_L^\#$ @ 15 °C (bar)	$P_H^\#$ @ 80 °C (bar)	$\ln(P_s/P_d)$	wt.% H ₂	Reference
1	Ti _{0.77} Zr _{0.3} Cr _{0.85} Fe _{0.7} Mn _{0.25} Ni _{0.2} Cu _{0.03}	93.7	19.3	25	110	–	1.6	[132]
2	Ti _{31.3} V _{13.2} Mn _{50.1} (Zr _{0.7} Cr _{1.4} Fe ₃)	109.3	24.7	17	113	0.54	1.53	[144]
3	Ti _{31.4} V _{15.2} Mn _{48.1} (Zr _{0.5} Cr _{1.3} Fe _{3.3})	107.8	24	19	120	0.52	1.35	[144]
4	Ti ₃₀ V _{15.8} Mn _{49.4} (Zr _{0.5} Cr _{1.1} Fe _{2.9})	109.5	24.3	21	133	0.57	1.6	[144]
5	(Ti _{0.85} Zr _{0.15}) _{1.1} Cr _{0.95} Mo _{0.05} Mn	115.2	26.2	18	138	–	1.88	[145]
6	(Ti _{0.85} Zr _{0.15}) _{1.1} Cr _{0.9} Mo _{0.1} Mn	106.4	23.7	18	112	–	1.78	[145]
7	(Ti _{0.85} Zr _{0.15}) _{1.1} Cr _{0.85} Mo _{0.15} Mn	100.9	21.7	22	115	–	1.67	[145]
8	(Ti _{0.85} Zr _{0.15}) _{1.1} Cr _{0.98} W _{0.02} Mn	113.8	26.3	15	113	–	1.52	[145]
9	(Ti _{0.85} Zr _{0.15}) _{1.1} Cr _{0.95} W _{0.05} Mn	109.2	24.3	20	128	–	1.43	[145]
10	(Ti _{0.85} Zr _{0.15}) _{1.1} Cr _{0.9} W _{0.1} Mn	106.2	22.6	28	160	–	1.36	[145]
11	Ti _{0.85} Zr _{0.17} Cr ₁ Mn _{0.2} Fe _{0.7} V _{0.1}	104.4	22.68	22	125	–	1.69	[146]
12	Ti _{0.85} Zr _{0.17} Cr _{0.9} Mn _{0.2} Fe _{0.8} V _{0.1}	102.8	21.22	33	170	–	1.65	[146]
13	Ti _{0.85} Zr _{0.17} Cr _{0.8} Mn _{0.2} Fe _{0.9} V _{0.1}	101.3	19.75	51	233	–	1.58	[146]
14	Ti _{0.82} Zr _{0.20} Cr _{0.9} Mn _{0.2} Fe _{0.8} V _{0.1}	103.4	22.2	24	130	–	1.68	[146]
15	Ti _{0.823} Zr _{0.17} Cr _{0.9} Mn _{0.2} Fe _{0.8} V _{0.1}	102.8	21.22	33	170	–	1.65	[146]
16	Ti _{0.826} Zr _{0.14} Cr _{0.9} Mn _{0.2} Fe _{0.8} V _{0.1}	102.4	20.14	50	234	–	1.64	[146]
17	Ti _{0.95} Zr _{0.05} Mn _{1.1} Cr _{0.7} V _{0.2}	97.1	21.27	16	84	0.07	1.81	[147]
18	Ti _{0.94} Zr _{0.06} Mn _{1.1} Cr _{0.7} V _{0.2}	99.8	22.36	14	80	0.1	1.82	[147]
19	Ti _{0.93} Zr _{0.07} Mn _{1.1} Cr _{0.7} V _{0.2}	100.3	22.86	12	72	0.07	1.83	[147]
20	Ti _{0.9} Zr _{0.1} Mn _{1.1} Cr _{0.7} V _{0.2}	97.9	22.92	9	53	0.07	1.88	[147]
21	Ti _{0.95} Zr _{0.05} Mn _{1.3} Cr _{0.5} V _{0.2}	97.2	21.18	17	88	0.22	1.84	[147]
22	Ti _{0.95} Zr _{0.05} Mn _{1.1} Cr _{0.7} V _{0.2}	97.1	21.27	16	84	0.07	1.81	[147]
23	Ti _{0.95} Zr _{0.05} Mn _{0.9} Cr _{0.9} V _{0.2}	97.4	21.64	14	76	0.02	1.78	[147]
24	(Ti _{0.9} Zr _{0.1}) _{1.125} Cr _{0.85} Mn _{1.1} Mo _{0.05}	110	24	25	157	–	1.48	[148]

efficiencies >60 % are desirable.

(2) Resilience to impurities, typically moisture and oxygen.

AB₂-type hydrides are particularly sensitive to moisture and oxygen contamination. In general, purification is standard downstream of the electrolyser. However, it may be beneficial to provide some level of additional protection. Much like AB₂ materials for buffer stores, hydrides can be reinforced with fluorine or mixed with polymers for additional resilience. A Ti-based AB₂ hydride was demonstrated to be affected by oxygen and carbon monoxide when concentration exceeds 10 ppm. Water also was shown to gradually reduce capacity. The results demonstrated that if the total contaminant content remains below 50 ppm, the hydride alloy exhibits sufficient cycle life for industrial applications [140].

(3) Minimising cost. This includes the base material cost, the material manufacturing cost, and the accompanying engineering components.

The base material cost depends on the elements used. For Ti-based AB₂ hydrides, Mn, Al, and Fe are cheap, Ti, Cr, Ni are medium cost, Zr, Mo, W & Co are high cost and V has a very high cost. The cost of V can be reduced by using alloys such as ferrovandium if the composition allows. This review details the behaviour of most of these elements [87], where in general one tries to produce an alloy with the cheapest elements while delivering the desired performance. A key aspect with AB₂ hydrides is the activation procedure, which is necessary to enable hydrogen cycling. Usually, adding more Ti to A-side and Cr to the B-side requires more aggressive activation conditions [87]. Another strategy is to incorporate lanthanum (La) in small quantities if Ni is present in the alloy. This creates LaNi₅ (an AB₅ material) that activates easily and

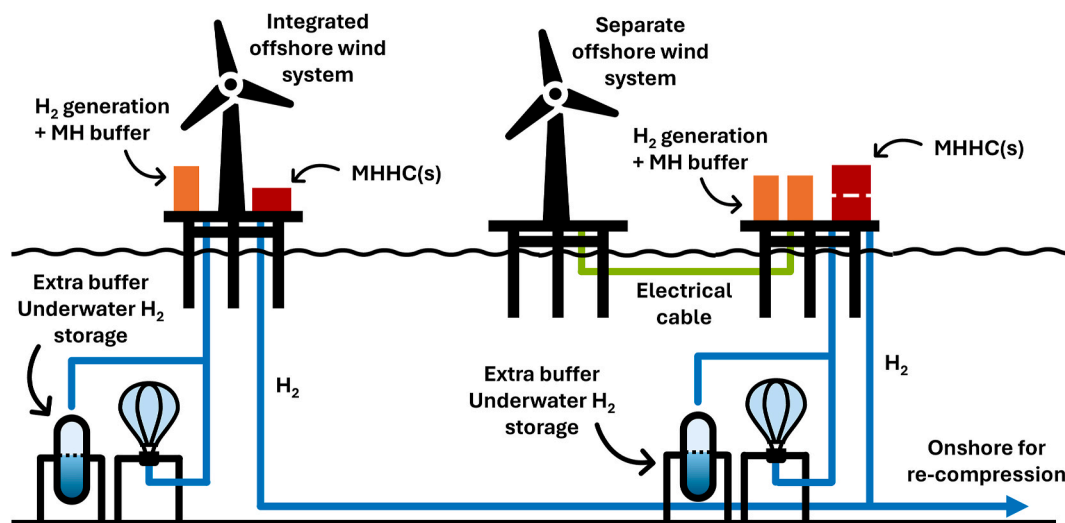


Fig. 8. Infographic of potential ways to improve offshore hydrogen systems. Both metal hydrides and underwater storage are used as buffer stores, whereas thermal compressors that utilise electrolyser waste heat push hydrogen to shore. Hydrogen is then re-compressed mechanically before storage or industry use.

allows the reaction to propagate [87]. The material manufacturing cost is covered in point (4) while the engineering design ties into point (1) and (5).

- (4) High scalability – other than cost, the alloy requires good ability for mass production, which exhibits similar performance at bulk scale compared to small gram samples.

An issue with titanium based AB₂-type hydrides is reproducing the hydride capability at tonnage scale. Ti-based alloys require processing temperatures >1600 °C, and at these temperatures, molten titanium exhibits high chemical activity. Furthermore, the additions to the base alloy also have their own unique processing temperatures, which need to be carefully considered to avoid inhomogeneity, stoichiometry issues and/or material vaporisation. As such, plasma skull melting (a variation of arc melting) with rapid quenching is used industrially [141,142], which adds a significant cost factor. It would be advantageous at medium to large scale to use vacuum induction melting (VIM), which is simple, allows homogenous stirring of the melt with a degree of good temperature control. The main challenge however is molten titanium reacting with the crucible material. This review extensively covers this [141]. In summary, important Ti-based AB₂ melts considerations are:

- Ti-based alloys are sensitive to non-metallic impurities, specifically oxygen. It is recommended to use de-oxidisers (La- or Ce-mischmetal, battery grade) during the melt, with the aim to keep the nominal oxygen content below 0.05 % by weight [140]. 2–3 wt% mischmetal is recommended [140].
 - Common MgO and Al₂O₃ crucibles will result in contamination of more than 1 wt% of oxygen. Y₂O₃ coated Al₂O₃ and MgO can reduce levels to ca. 0.05 wt%, but then there are issues of coating durability. Other options are AlN and BaZrO₃ crucibles [141]. A recent study examining AlN crucibles for TiNi melts found AlN crucibles feasible for induction melting of TiNi alloys [143].
 - Pre-alloy the less aggressive components (Mn, Fe, V) before melting again with the remaining elements (Ti, Zr, Cr) plus de-oxidiser [87,132].
 - Rapid cooling of the melt at large scale is essential for stabilizing the C14 phase. Cooling speeds of around 10 K s⁻¹ are recommended [140].
- (5) Enabling high flow compressors suitable for industrial applications.

Ensuring high performance efficiency and elevated delivery rates poses a pivotal requirement for large-scale MHHCs. However, this becomes particularly challenging due to the inherent difficulty of efficiently transferring heat to and from a hydride, primarily attributed to the low thermal conductivity of powders, as discussed earlier. Typically, this results in compressors with small radii and considerable lengths, limiting the dimensions and scalability. Furthermore, the scale-up of compressors introduces challenges associated with increased material usage. Consequently, a key obstacle lies in the development of scalable designs that minimise material usage while effectively addressing the heat transfer constraints.

4.2. Integration of oxyfuel processes and thermal compressors into large-scale hydrogen storage

Large-scale hydrogen storage involves four stages: generation, compression, storage, and utilisation (e.g., power and/or heat). Power generation can be achieved via various means, such as gas turbines, 4-stroke engines, or fuel cells [26]. The generation and power units exhibit the highest energy losses within the entire process, meriting focused efforts for improvement. Enhancements can stem from advancements within individual technologies, such as electrolyzers. Alternatively, optimising integration is another prospective area,

discussed within this section.

For example, if a gas turbine is used, the open system Brayton cycle consists of a compressor, a combustion chamber, and a turbine. In natural gas turbines, air is compressed, combined with natural gas, combusted, and expanded through a turbine [149]. Many gas turbines converted to hydrogen follow a similar concept. On many occasions, a steam Rankine cycle is integrated within a Brayton cycle for additional useful work (combined cycle) [150]. This has disadvantages such as nitrogen oxide(s) (NO_x) formation and a low-pressure ratio. Studies have attempted to mitigate the nitrogen oxide content through various combustion design and operation strategies [151,152].

One method to increase the Brayton cycle efficiency is to increase the compression pressure ratio [149]. If oxygen is stored from electrolysis, then the combustion chamber can run via an oxyfuel process, removing the nitrogen component, and enabling higher pressure ratios. A study proposing oxyfuel and an integration of the Brayton and Rankine cycle, named the Graz Cycle, resulted in a net efficiency of 68.5 % (LHV), using oxygen, hydrogen, and re-injection of steam at an inlet pressure of 40 bar to the combustion chamber [153]. A diagram of the Graz cycle is reproduced in Fig. 9.

Furthermore, the oxyfuel process means the electrolysis acts as the “first” compression stage, as the electrolyser compresses water from 1 to 30 bar and conveniently separates the gases. At the second compression stage, the waste heat from the electrolyser can be utilised to thermally compress the hydrogen, from 30 to ca. 100 bar. A third compression stage (either thermal or mechanical) to ca. 250 bar can be employed to reach top-end underground storage pressures if required. The oxygen is assumed mechanically compressed, rather than stored as a liquid. If there was a minimum cushion gas storage pressure of ca. 90 bar, and if technically possible, then the compressed gas can be combusted and sent through the turbine at very-high pressure ratios. Note, thermal compressors are in early-stage research development, and oxyfuel gas turbines are not readily available (to the author’s knowledge), but every other unit/process are either available in the market, or near deployment.

For comparison, the inclusion of an oxyfuel process and MHHC(s) on the overall roundtrip efficiency (LHV) of large-scale hydrogen storage is shown in Fig. 10. A simple H₂ generation, compression, and power generation with a combined cycle (CC), results in an efficiency of 37 %. This is based on an electrolyser consumption of 54 kW h kg H₂⁻¹ [57, 131], and a turbine (CC) efficiency of 63 % (1600 °C class GT) [154]. An oxyfuel process (Graz 68.5 % [153]) with mechanical compression improves this to 40 %, with 1 MHHC increasing it to 41 %, and 2 MHHCs increasing it further to 42 %. The 1 MHHC case is based on 60 % efficiency and the 2 MHHC case is based on a 80 % efficient MHHC (performance efficiency). If an electrolyser consumption of 52.5 kW h kg H₂⁻¹ is assumed (and this reduction comes from the balance of plant rather than stack improvements), the roundtrip efficiency is 43 %.

If an oxyfuel power generation option is adopted, storing both oxygen and hydrogen is necessary. The additional cost of oxygen storage, compression and piping would also need to be considered, especially if the hydrogen is made offshore. It is conceivable however, that hydrogen made far offshore and transported to land is earmarked for industry, while hydrogen (and oxygen) produced on land is prioritised for energy storage. Underground storage of gaseous oxygen has been investigated [155], but not yet demonstrated, while oxygen can also be stored as a liquid, albeit there will be a significant energy requirement to do so. Considering the power generation options, gas turbines (combined cycle - CC) are a mature and expensive technology at 1084 USD/kW [156], whereas polymer electrolyte membrane (PEM) fuel cells and 4-stroke engines are 900 USD/kW and 400 USD/kW respectively [156]. As fuel cell efficiency can be increased by 10–15% using an oxyfuel process (and 1 atm operating pressure), it might be more beneficial in the long-term to adopt fuel cells/4-stroke engines [156], as these options although may not exhibit as high efficiencies as oxyfuel turbines (CC), they are significantly cheaper while attaining good efficiencies.

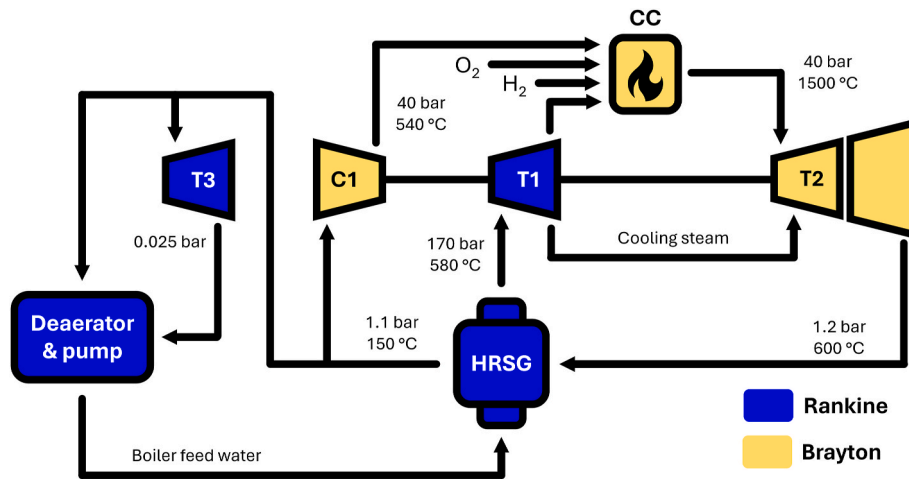


Fig. 9. Flow scheme of Graz Cycle (reproduced) [153]. Rankine = High pressure steam turbine (T1), low pressure steam turbine (T3) and heat recovery steam generator (HRSG). Brayton = Compressor (C1), combustion chamber (CC) and high temperature turbine (T2).

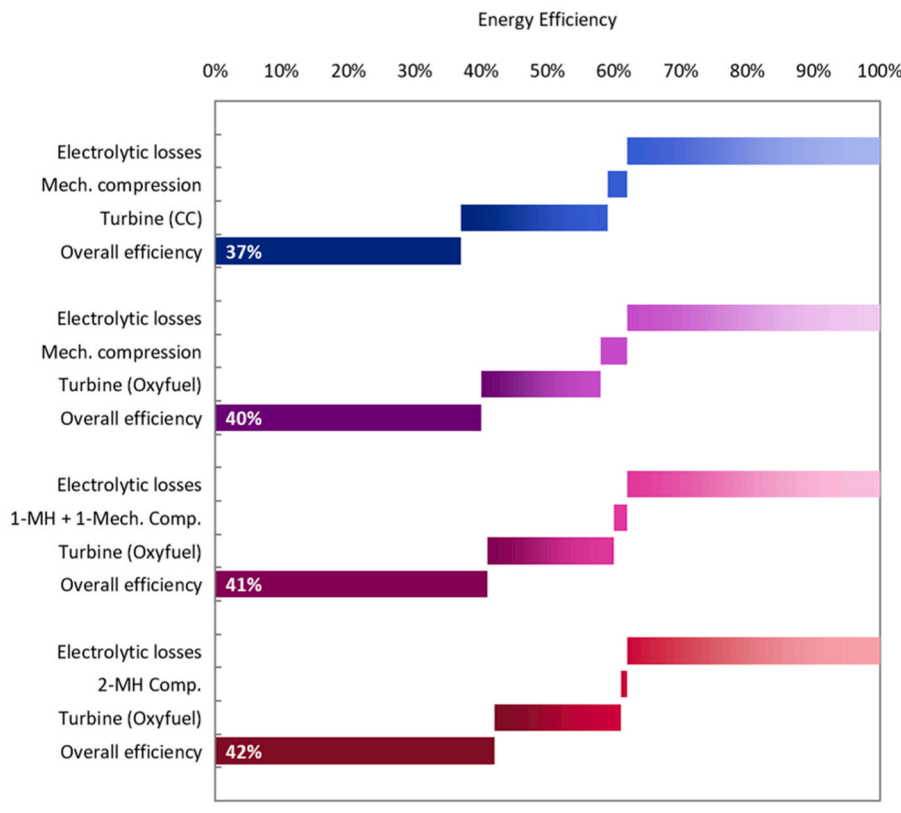


Fig. 10. Waterfall chart of approximate cycle efficiencies outlining the potential of MHCs and oxyfuel within a combined cycle. Efficiencies based on LHV for both electrolysis and turbine. (CC – combined cycle, oxyfuel = Graz cycle).

5. Conclusion

This article reviews the literature surrounding onshore and offshore large-scale hydrogen storage, focusing primarily on the storage, compression and roundtrip efficiency aspects. Consequently, proposed future perspectives and potential research avenues have been identified to provide technological advances to large-scale hydrogen storage.

Large-scale hydrogen storage has emerged as a compelling option to store energy at a TWh scale. Considering offshore wind installations, the question of when hydrogen should be produced offshore or on land, does not hold a definitive answer at present, however a DNV report states a

transition distance of 100–150 km. With decreasing costs in green hydrogen production and a potential realisation in hydrogen thermal compression, offshore H₂ production will become more attractive, especially as H₂ pipelines are cheaper than electrical cables, have easier environmental approval processes, and lower transmission losses.

Underground hydrogen storage has been widely recognised as a competitive method to store large volumes of hydrogen for months to years. On the TWh scale, storing hydrogen in underground stores is an order of magnitude less than the cost of storage in high pressure tanks or as a liquid. Onshore installations are more cost effective than offshore, with storage options chosen based on duration, rate of discharge,

geographic availability, and cost. Onshore salt caverns have been recognised as the cheapest underground hydrogen storage solution at 7 GBP/kg H₂⁻¹, although geographic availability is limited. Regarding the UK, the East Yorkshire basin has been recognised as a suitable location to store surplus energy supplied by offshore North Sea installations.

Metal hydrides are not suitable for large-scale hydrogen storage, due to high material costs, but have potential in next generation “hybrid” buffer stores, enabling 6 times or greater improved hydrogen density compared to compressed gas alone. Underwater hydrogen storage, either in fixed or flexible walled structures, may find use as additional buffer storage in deepwater offshore wind installations (300–400 m depth). As the hydrostatic pressure from water depth is utilised, the nominal wall containment allows inexpensive vessel costs, and allows tethering above the sea floor, reducing effect to marine life. Metal hydrides may also find application in slurries for hydrogen transport but require further study.

Metal hydride hydrogen compressors (MHHCs) can improve the roundtrip efficiency of large-scale hydrogen storage by utilising electrolyser waste heat. With 80 % assumed performance efficiency, up to 2 MHHCs are possible, potentially enabling compression up to 500+ bar and completely replacing mechanical compression of hydrogen. Regarding offshore installations, MHHCs can act as first stage compressors, transporting hydrogen to land for subsequent re-compression for storage or industry use. First-stage MHHC materials available in the literature are suitable for prototypes, with extra optimisation possible for the 1st stage, and required for 2nd and 3rd stage compressors. The engineering of MHHC prototypes need significant improvement to enable utilisation in industrial processes. Areas to focus on are progress in thermodynamic theory, plus exploration and demonstration of ways to enable high flow compression while minimising MH material.

Utilising an oxyfuel process by also storing oxygen from electrolysis can improve the roundtrip efficiency of large-scale hydrogen storage, by enabling higher pressure ratios (for gas turbines) and removing the nitrogen component, thereby eliminating NO_x emissions. The overall efficiency is improved by 3 % compared to a traditional combined cycle process. With the addition of a 2-stage MHHC, the overall efficiency can approach 42 %, based on an electrolyser consumption of 54 kW h kg H₂⁻¹. With additional advancements in electrolyser efficiencies, up to 43 % roundtrip efficiency may be achievable.

CRediT authorship contribution statement

Marcus J. Adams: Writing – review & editing, Writing – original draft, Visualization, Resources, Methodology, Investigation, Formal analysis, Data curation, Conceptualization. **Matthew D. Wadge:** Writing – review & editing, Writing – original draft, Visualization. **Drew Sheppard:** Writing – review & editing, Writing – original draft. **Alastair Stuart:** Validation, Supervision, Project administration, Funding acquisition. **David M. Grant:** Writing – review & editing, Validation, Supervision, Funding acquisition.

Declaration of generative AI and AI-assisted technologies in the writing process

During the preparation of this work the author(s) used ChatGPT 3.5 in order to act as an internal reviewer, specifically for grammar enhancements and English optimisation (i.e. more efficient paragraphs/sentences). Questions asked to ChatGPT typically were “can you improve this?”, or “can you reduce the word count?”. After using this tool/service, the author(s) reviewed and edited the content as needed and take(s) full responsibility for the content of the publication.

Declaration of competing interest

The authors declare that they have no known competing financial interests or personal relationships that could have appeared to influence

the work reported in this paper.

The authors declare the following financial interests/personal relationships which may be considered as potential competing interests: Marcus Adams reports financial support was provided by Engineering and Physical Sciences Research Council. If there are other authors, they declare that they have no known competing financial interests or personal relationships that could have appeared to influence the work reported in this paper.

Acknowledgements

This work was funded through Engineering and Physical Sciences Research Council (EPSRC) [grant number EP/W005131/1] and is part of the Ocean Renewable Energy Fuel (Ocean-REFuel) project.

References

- [1] Service CCC. Global climate highlights 2023. <https://climate.copernicus.eu/global-climate-highlights-2023>; 2023.
- [2] Dixon J, Bell K, Brush S. Which way to net zero? a comparative analysis of seven UK 2050 decarbonisation pathways. *Renew Sustain Energy Transit* 2022;2: 100016. <https://doi.org/10.1016/j.rset.2021.100016>.
- [3] Faye O, Szpunar J, Eduok U. A critical review on the current technologies for the generation, storage, and transportation of hydrogen. *Int J Hydrogen Energy* 2022; 47:13771–802. <https://doi.org/10.1016/j.ijhydene.2022.02.112>.
- [4] Yue M, Lambert H, Pahon E, Roche R, Jemei S, Hissel D. Hydrogen energy systems: a critical review of technologies, applications, trends and challenges. *Renew Sustain Energy Rev* 2021;146:111180. <https://doi.org/10.1016/j.rser.2021.111180>.
- [5] Abdalla AM, Hossain S, Nisfindy OB, Azad AT, Dawood M, Azad AK. Hydrogen production, storage, transportation and key challenges with applications: a review. *Energy Convers Manag* 2018;165:602–27. <https://doi.org/10.1016/j.enconman.2018.03.088>.
- [6] Tashie-Lewis BC, Nnabuife SG. Hydrogen production, distribution, storage and power conversion in a hydrogen economy - a technology review. *Chem Eng J Adv* 2021;8:100172. <https://doi.org/10.1016/j.cej.2021.100172>.
- [7] Ratnakar RR, Gupta N, Zhang K, van Doorne C, Fesmire J, Dindoruk B, et al. Hydrogen supply chain and challenges in large-scale LH2 storage and transportation. *Int J Hydrogen Energy* 2021;46:24149–68. <https://doi.org/10.1016/j.ijhydene.2021.05.025>.
- [8] Sazali N. Emerging technologies by hydrogen: a review. *Int J Hydrogen Energy* 2020;45:18753–71. <https://doi.org/10.1016/j.ijhydene.2020.05.021>.
- [9] Muthukumar P, Kumar A, Afzal M, Bhogilla S, Sharma P, Parida A, et al. Review on large-scale hydrogen storage systems for better sustainability. *Int J Hydrogen Energy* 2023;48:33223–59. <https://doi.org/10.1016/j.ijhydene.2023.04.304>.
- [10] Hassan IA, Ramadan HS, Saleh MA, Hissel D. Hydrogen storage technologies for stationary and mobile applications: review, analysis and perspectives. *Renew Sustain Energy Rev* 2021;149:111311. <https://doi.org/10.1016/j.rser.2021.111311>.
- [11] Zheng J, Zhou H, Wang C-G, Ye E, Xu JW, Loh XJ, et al. Current research progress and perspectives on liquid hydrogen rich molecules in sustainable hydrogen storage. *Energy Storage Mater* 2021;35:695–722. <https://doi.org/10.1016/j.ensm.2020.12.007>.
- [12] ullah Rather S. Preparation, characterization and hydrogen storage studies of carbon nanotubes and their composites: a review. *Int J Hydrogen Energy* 2020; 45:4653–72. <https://doi.org/10.1016/j.ijhydene.2019.12.055>.
- [13] Zarezadeh Mehrizi M, Abdi J, Rezakazemi M, Salehi E. A review on recent advances in hollow spheres for hydrogen storage. *Int J Hydrogen Energy* 2020;45: 17583–604. <https://doi.org/10.1016/j.ijhydene.2020.04.201>.
- [14] Abe JO, Popoola API, Ajenifuja E, Popoola OM. Hydrogen energy, economy and storage: review and recommendation. *Int J Hydrogen Energy* 2019;44:15072–86. <https://doi.org/10.1016/j.ijhydene.2019.04.068>.
- [15] Moradi R, Groth KM. Hydrogen storage and delivery: review of the state of the art technologies and risk and reliability analysis. *Int J Hydrogen Energy* 2019;44: 12254–69. <https://doi.org/10.1016/j.ijhydene.2019.03.041>.
- [16] Andersson J, Grönkvist S. Large-scale storage of hydrogen. *Int J Hydrogen Energy* 2019;44:11901–19. <https://doi.org/10.1016/j.ijhydene.2019.03.063>.
- [17] Preuster P, Alekseev A, Wasserscheid P. Hydrogen storage technologies for future energy systems. *Annu Rev Chem Biomol Eng* 2017;8:445–71. <https://doi.org/10.1146/annurev-chembioeng-060816-101334>.
- [18] Fan L, Tu Z, Chan SH. Recent development of hydrogen and fuel cell technologies: a review. *Energy Rep* 2021;7:8421–46. <https://doi.org/10.1016/j.egy.2021.08.003>.
- [19] Odenweller A, Ueckerdt F, Nemet GF, Jensterle M, Luderer G. Probabilistic feasibility space of scaling up green hydrogen supply. *Nat Energy* 2022;7:854–65. <https://doi.org/10.1038/s41560-022-01097-4>.
- [20] Durakovic G, del Granado PC, Tomasgard A. Powering Europe with North Sea offshore wind: the impact of hydrogen investments on grid infrastructure and power prices. *Energy* 2023;263:125654. <https://doi.org/10.1016/j.energy.2022.125654>.

- [21] Galparsoro I, Menchaca I, Garmendia JM, Borja A, Maldonado AD, Iglesias G, et al. Reviewing the ecological impacts of offshore wind farms. *Npj Ocean Sustain* 2022;1:1. <https://doi.org/10.1038/s44183-022-00003-5>.
- [22] Jiang Z. Installation of offshore wind turbines: a technical review. *Renew Sustain Energy Rev* 2021;139:110576. <https://doi.org/10.1016/j.rser.2020.110576>.
- [23] Cranmer A, Broughel AE, Ericson J, Goldberg M, Dharni K. Getting to 30 GW by 2030: visual preferences of coastal residents for offshore wind farms on the US East Coast. *Energy Pol* 2023;173:113366. <https://doi.org/10.1016/j.enpol.2022.113366>.
- [24] Harrison RM, Clarke AG, Tomlin AS. The atmosphere. In: Harrison RM, editor. *Underst. Our environ. An introd. To environ. Chem. Pollut. The Royal Society of Chemistry*; 1999. <https://doi.org/10.1039/9781847552235-00009>.
- [25] Ramakrishnan S, Delpisheh M, Convery C, Niblett D, Vinothkannan M, Mamlouk M. Offshore green hydrogen production from wind energy: critical review and perspective. *Renew Sustain Energy Rev* 2024;195:114320. <https://doi.org/10.1016/j.rser.2024.114320>.
- [26] Society TR. *Large-scale electricity storage*. 2023.
- [27] International Energy Agency. *Net zero by 2050: a roadmap for the global energy sector*. 2021.
- [28] Elberry AM, Thakur J, Santasalo-Aarnio A, Larmi M. Large-scale compressed hydrogen storage as part of renewable electricity storage systems. *Int J Hydrogen Energy* 2021;46:15671–90. <https://doi.org/10.1016/j.ijhydene.2021.02.080>.
- [29] IEA. *The future of hydrogen*. 2019. Paris.
- [30] Wang A, Jens J, Mavins D, Moultak M, Schimmel M, Van Der Leun K, et al. *Guidehouse: analysing future demand, supply, and transport of hydrogen*. 2021.
- [31] Tsiklivos C, Hermesmann M, Müller TE. Hydrogen transport in large-scale transmission pipeline networks: thermodynamic and environmental assessment of repurposed and new pipeline configurations. *Appl Energy* 2022;327:120097. <https://doi.org/10.1016/j.apenergy.2022.120097>.
- [32] Kimtantis CL, Taylor MA. An effective solution for elemental sulfur deposition in natural gas systems. 2014 Conf. Proc. Oil Gas Chem. Filtr. Sep. AFS 2014;2014: 216–26.
- [33] Someday BP, Marchi CSAN. 3 - hydrogen containment materials. In: Walker GBT-S-SHS, editor. *Woodhead publ. Ser. Electron. Opt. Mater. Woodhead Publishing*; 2008. p. 51–81. <https://doi.org/10.1533/9781845694944.1.51>.
- [34] Penev M, Zuboy J, Hunter C. Economic analysis of a high-pressure urban pipeline concept (HyLine) for delivering hydrogen to retail fueling stations. *Transport Res Transport Environ* 2019;77:92–105. <https://doi.org/10.1016/j.trd.2019.10.005>.
- [35] Walker G. *Solid-state hydrogen storage*. first ed. Woodhead Publishing; 2008.
- [36] Yu Q, Hao Y, Ali K, Hua Q, Sun L. Techno-economic analysis of hydrogen pipeline network in China based on levelized cost of transportation. *Energy Convers Manag* 2024;301:118025. <https://doi.org/10.1016/j.enconman.2023.118025>.
- [37] Wasim M, Djukic MB. External corrosion of oil and gas pipelines: a review of failure mechanisms and predictive preventions. *J Nat Gas Sci Eng* 2022;100: 104467. <https://doi.org/10.1016/j.jngse.2022.104467>.
- [38] Grigat N, Mölling T, Torres Crooks SJ, Vollbrecht B, Sackmann J, Gries T. Investigation of cost-effective braided and wound composite pipelines for hydrogen applications. <https://doi.org/10.1115/IPC2022-87191>; 2022.
- [39] Lamb KE, Webb CJ. A quantitative review of slurries for hydrogen storage – slush hydrogen, and metal and chemical hydrides in carrier liquids. *J Alloys Compd* 2022;906:164235. <https://doi.org/10.1016/j.jallcom.2022.164235>.
- [40] McClaine AW, Brown K, Bowen DDG. Magnesium hydride slurry: a better answer to hydrogen storage. *J Energy Resour Technol Trans ASME* 2015;137. <https://doi.org/10.1115/1.4030398>.
- [41] Snijder ED, Versteeg GF, van Swaaij WPM. Kinetics of hydrogen absorption and desorption in LaNi₅-xAlx slurries. *AICHE J* 1993;39:1444–54. <https://doi.org/10.1002/aic.690390904>.
- [42] Tung Y, Grohse EW, Hill FB. Kinetics of hydrogen absorption in a stirred metal hydride slurry. *AICHE J* 1986;32:1821–31. <https://doi.org/10.1002/aic.690321107>.
- [43] Brown K, McClaine A, Bowen D. Hydrogen and a new paradigm for electricity storage. In: 2019 offshore energy storage summit; 2019. p. 1–10. <https://doi.org/10.1109/OSES.2019.8867077>.
- [44] Goodell PD, Sandrock GD, Huston EL. Microstructure and hydriding studies of AB/sub 5/hydrogen storage compounds. United States: Final report; 1980. <https://doi.org/10.2172/5568617>.
- [45] Lamb KE, Webb CJ. A quantitative review of slurries for hydrogen storage – slush hydrogen, and metal and chemical hydrides in carrier liquids. *J Alloys Compd* 2022;906:164235. <https://doi.org/10.1016/j.jallcom.2022.164235>.
- [46] Ji D, Liu G, Romagnoli A, Rajoo S, Besagni G, Markides CN. Low-grade thermal energy utilization: technologies and applications. *Appl Therm Eng* 2024;244: 122618. <https://doi.org/10.1016/j.applthermaleng.2024.122618>.
- [47] Yabuki A, Sugita K, Matsumura M, Hirashima M, Tsunaga M. The anti-slurry erosion properties of polyethylene for sewerage pipe use. *Wear* 2000;240:52–8. [https://doi.org/10.1016/S0043-1648\(00\)00343-4](https://doi.org/10.1016/S0043-1648(00)00343-4).
- [48] Wassenaar J, Micic P. *HDPE pipe is hydrogen ready - white paper*. Altona; 2020.
- [49] Aziz M. Liquid hydrogen: a review on liquefaction, storage, transportation, and safety. *Energies* 2021;14. <https://doi.org/10.3390/en14185917>.
- [50] Aasadnia M, Mehrpooya M. Large-scale liquid hydrogen production methods and approaches: a review. *Appl Energy* 2018;212:57–83. <https://doi.org/10.1016/j.apenergy.2017.12.033>.
- [51] Van Hoecke L, Laffineur L, Campe R, Perreault P, Verbruggen SW, Lenaerts S. Challenges in the use of hydrogen for maritime applications. *Energy Environ Sci* 2021;14:815–43. <https://doi.org/10.1039/D0EE01545H>.
- [52] Kawasaki. Liquefied hydrogen carrier - SUIISO FRONTIER- receives classification from nippon kaiji kyokai. https://global.kawasaki.com/en/corp/newsroom/news/detail/?f=202111203_9557. [Accessed 7 May 2024].
- [53] BNEF. *Hydrogen economy Outlook*. 2020.
- [54] Kurien C, Mittal M. Utilization of green ammonia as a hydrogen energy carrier for decarbonization in spark ignition engines. *Int J Hydrogen Energy* 2023;48: 28803–23. <https://doi.org/10.1016/j.ijhydene.2023.04.073>.
- [55] Ishaq H, Crawford C. Review and evaluation of sustainable ammonia production, storage and utilization. *Energy Convers Manag* 2024;300:117869. <https://doi.org/10.1016/j.enconman.2023.117869>.
- [56] International Energy Agency. *Ammonia Technology Roadmap towards more sustainable nitrogen fertiliser production*. 2021.
- [57] Pfromm PH. Towards sustainable agriculture: fossil-free ammonia. *J Renew Sustain Energy* 2017;9. <https://doi.org/10.1063/1.4985090>.
- [58] Smith C, Hill AK, Torrente-Murciano L. Current and future role of Haber-Bosch ammonia in a carbon-free energy landscape. *Energy Environ Sci* 2020;13:331–44. <https://doi.org/10.1039/c9ee02873k>.
- [59] Humphreys J, Lan R, Tao S. Development and recent progress on ammonia synthesis catalysts for haber–bosch process. *Adv Energy Sustain Res* 2021;2: 2000043. <https://doi.org/10.1002/aesr.202000043>.
- [60] Lucentini I, Garcia X, Vendrell X, Llorca J. Review of the decomposition of ammonia to generate hydrogen. *Ind Eng Chem Res* 2021;60:18560–611. <https://doi.org/10.1021/acs.iecr.1c00843>.
- [61] Verschuur J, Salmon N, Hall J, Bañares-Alcántara R. Optimal fuel supply of green ammonia to decarbonise global shipping. *Environ Res Infrastruct Sustain* 2024;4: 15001. <https://doi.org/10.1088/2634-4505/ad097a>.
- [62] Niermann M, Beckendorff A, Kaltschmitt M, Bonhoff K. Liquid organic hydrogen carrier (LOHC) – assessment based on chemical and economic properties. *Int J Hydrogen Energy* 2019;44:6631–54. <https://doi.org/10.1016/j.ijhydene.2019.01.199>.
- [63] Chu C, Wu K, Luo B, Cao Q, Zhang H. Hydrogen storage by liquid organic hydrogen carriers: catalyst, renewable carrier, and technology – a review. *Carbon Resour Convers* 2023;6:334–51. <https://doi.org/10.1016/j.crcon.2023.03.007>.
- [64] Brückner N, Obesser K, Bösmann A, Teichmann D, Arlt W, Dungs J, et al. Evaluation of industrially applied heat-transfer fluids as liquid organic hydrogen carrier systems. *ChemSusChem* 2014;7:229–35. <https://doi.org/10.1002/cssc.201300426>.
- [65] Patonia A, Lenivova V, Poudineh R, Nolden C. Hydrogen pipelines vs. HVDC lines : should we transfer green molecules or electrons? Oxford; 2023.
- [66] Van Wingerden T, Geerdink D, Taylor C, Hülsen CF. Specification of a European offshore hydrogen backbone. 2023.
- [67] Miao B, Giordano L, Chan SH. Long-distance renewable hydrogen transmission via cables and pipelines. *Int J Hydrogen Energy* 2021;46:18699–718. <https://doi.org/10.1016/j.ijhydene.2021.03.067>.
- [68] Calado G, Castro R. Hydrogen production from offshore wind parks: current situation and future perspectives. *Appl Sci* 2021;11. <https://doi.org/10.3390/app11225561>.
- [69] Kruck O, Prelicz R, Rudolph T, Crotofino F. HyUnder project - D3.1 overview on all known underground storage technologies for hydrogen. Walqa; 2013.
- [70] Crotofino F, Landinger H, Bünger U, Raksha T, Simon J, Correas L. Update of Benchmarking of large scale hydrogen underground storage with competing options. 2014.
- [71] Hematpur H, Abdollahi R, Rostami S, Haghighi M, Blunt MJ. Review of underground hydrogen storage: concepts and challenges. *Adv Geo-Energy Res* 2023;7:111–31. <https://doi.org/10.46690/ager.2023.02.05>.
- [72] Muhammed NS, Haq B, Al Shehri D, Al-Ahmed A, Rahman MM, Zaman E. A review on underground hydrogen storage: insight into geological sites, influencing factors and future outlook. *Energy Rep* 2022;8:461–99. <https://doi.org/10.1016/j.egyrs.2021.12.002>.
- [73] Epelle EI, Obande W, Udourioh GA, Afolabi IC, Desongu KS, Orivri U, et al. Perspectives and prospects of underground hydrogen storage and natural hydrogen. *Sustain Energy Fuels* 2022;6:3324–43. <https://doi.org/10.1039/d2se00618a>.
- [74] Williams JDO, Williamson JP, Parkes D, Evans DJ, Kirk KL, Sunny N, et al. Does the United Kingdom have sufficient geological storage capacity to support a hydrogen economy? Estimating the salt cavern storage potential of bedded halite formations. *J Energy Storage* 2022;53:105109. <https://doi.org/10.1016/j.est.2022.105109>.
- [75] Energy Technologies Institute. Hydrogen: the role of hydrogen storage in a clean responsive power system. *Energy Technol Inst* 2015;11. <http://www.eti.co.uk/wp-content/uploads/2015/05/3380-ETI-Hydrogen-Insights-paper.pdf>. [Accessed 3 January 2023].
- [76] Smith NJP, Evans DJ, Andrew I. The geology of gas storage in offshore salt caverns. *Mar Coast Hydrocarb Program Br Geol Surv* 2005:1–22.
- [77] Tingle M. Salting away our spare gas. *R Soc Chem* 2012. <https://edu.rsc.org/feature/salting-away-our-spare-gas/2020226>. [Accessed 10 March 2024].
- [78] Panagopoulos A, Haralambous KJ, Loizidou M. Desalination brine disposal methods and treatment technologies - a review. *Sci Total Environ* 2019;693: 133545. <https://doi.org/10.1016/j.scitotenv.2019.07.351>.
- [79] Caglayan DG, Weber N, Heinrichs HU, Linßen J, Robinus M, Kukla PA, et al. Technical potential of salt caverns for hydrogen storage in Europe. *Int J Hydrogen Energy* 2020;45:6793–805. <https://doi.org/10.1016/j.ijhydene.2019.12.161>.
- [80] Amid A, Mignard D, Wilkinson M. Seasonal storage of hydrogen in a depleted natural gas reservoir. *Int J Hydrogen Energy* 2016;41:5549–58. <https://doi.org/10.1016/j.ijhydene.2016.02.036>.

- [81] Gautier DL. Kimmeridgian shales total petroleum system of the North Sea graben province. 2005.
- [82] WindEurope. European offshore wind farms map public 2022. <https://windeurope.org/intelligence-platform/product/european-offshore-wind-farms-map-public/>. [Accessed 3 January 2023].
- [83] Wang Q, Qin H, Jia L, Li Z, Zhang G, Li Y, et al. Failure prediction and optimization for composite pressure vessel combining FEM simulation and machine learning approach. *Compos Struct* 2024;337:118099. <https://doi.org/10.1016/j.compstruct.2024.118099>.
- [84] Cai W, Li C, Agbossou K, Bénard P, Xiao J. A review of hydrogen-based hybrid renewable energy systems: simulation and optimization with artificial intelligence. *J Phys Conf Ser* 2022;2208:12012. <https://doi.org/10.1088/1742-6596/2208/1/012012>.
- [85] Rivard E, Trudeau M, Zaghbi K. Hydrogen storage for mobility: a review. *Materials* 2019;12. <https://doi.org/10.3390/ma12121973>.
- [86] Yartys VA, Lototsky MV, Akiba E, Albert R, Antonov VE, Ares JR, et al. Magnesium based materials for hydrogen based energy storage: past, present and future. *Int J Hydrogen Energy* 2019;44:7809–59. <https://doi.org/10.1016/j.ijhydene.2018.12.212>.
- [87] Yartys VA, Lototsky MV. Laves type intermetallic compounds as hydrogen storage materials: a review. *J Alloys Compd* 2022;916:165219. <https://doi.org/10.1016/j.jallcom.2022.165219>.
- [88] Radtke G, Dresselhaus M, Chen G, Be V. Size effects on the hydrogen storage properties of nanostructured metal hydrides: a review. *Int J Energy Res* 2007. <https://doi.org/10.1002/er>.
- [89] Modi P, Aguey-Zinsou K-F. Titanium-iron-manganese (TiFe_{0.85}Mn_{0.15}) alloy for hydrogen storage: reactivation upon oxidation. *Int J Hydrogen Energy* 2019;44:16757–64. <https://doi.org/10.1016/j.ijhydene.2019.05.005>.
- [90] Tarasov BP, Fursikov PV, Volodin AA, Bocharnikov MS, Shimkus YY, Kashin AM, et al. Metal hydride hydrogen storage and compression systems for energy storage technologies. *Int J Hydrogen Energy* 2021;46:13647–57. <https://doi.org/10.1016/j.ijhydene.2020.07.085>.
- [91] Bishnoi A, Sharma P. Large-scale production of BCC solid solution hydrogen storage alloy. *Int J Hydrogen Energy* 2024. <https://doi.org/10.1016/j.ijhydene.2024.01.301>.
- [92] Bernauer O, Töpler J, Noréus D, Hempelmann R, Richter D. Fundamentals and properties of some Ti/Mn based Laves phase hydrides. *Int J Hydrogen Energy* 1989;14:187–200. [https://doi.org/10.1016/0360-3199\(89\)90053-0](https://doi.org/10.1016/0360-3199(89)90053-0).
- [93] Bowman RC, Craft BD, Attalla A, Johnson JR. Diffusion behavior in titanium-chromium hydrides. *Int J Hydrogen Energy* 1983;8:801–8. [https://doi.org/10.1016/0360-3199\(83\)90211-2](https://doi.org/10.1016/0360-3199(83)90211-2).
- [94] Hatrick-Simpers JR, Choudhary K, Corgnale C. A simple constrained machine learning model for predicting high-pressure-hydrogen-compressor materials. *Mol Syst Des Eng* 2018;3:509–17. <https://doi.org/10.1039/C8ME00005K>.
- [95] Witman MD, Ling S, Wadge M, Bouzidi A, Pineda-Romero N, Clulow R, et al. Towards Pareto optimal high entropy hydrides via data-driven materials discovery. *J Mater Chem A* 2023;11:15878–88. <https://doi.org/10.1039/D3TA02323K>.
- [96] Kumar A, Tiwari S, Gupta N, Sharma P. Machine learning modelling and optimization for metal hydride hydrogen storage systems. *Sustain Energy Fuels* 2024;8:2073–86. <https://doi.org/10.1039/D4SE00031E>.
- [97] Tiwari S, Gupta N, Kumar S, Kumar A, Sharma P. Experimental investigation, development of machine learning model and optimization studies of a metal hydride reactor with embedded helical cooling tube. *J Energy Storage* 2023;72:108522. <https://doi.org/10.1016/j.est.2023.108522>.
- [98] Fruchart D, Soubeyroux JL, Hempelmann R. Neutron diffraction in Ti_{1.2}Mn_{1.8} deuteride: structural and magnetic aspects. *J Less Common Met* 1984;99:307–19. [https://doi.org/10.1016/0022-5088\(84\)90229-7](https://doi.org/10.1016/0022-5088(84)90229-7).
- [99] Endo N, Shimoda E, Goshome K, Yamane T, Nozu T, Maeda T. Construction and operation of hydrogen energy utilization system for a zero emission building. *Int J Hydrogen Energy* 2019;44:14596–604. <https://doi.org/10.1016/j.ijhydene.2019.04.107>.
- [100] Cui Y, Zeng X, Xiao J, Kou H. The comprehensive review for development of heat exchanger configuration design in metal hydride bed. *Int J Hydrogen Energy* 2022;47:2461–90. <https://doi.org/10.1016/j.ijhydene.2021.10.172>.
- [101] Ahluwalia RK. Sodium alanate hydrogen storage system for automotive fuel cells. *Int J Hydrogen Energy* 2007;32:1251–61. <https://doi.org/10.1016/j.ijhydene.2006.07.027>.
- [102] Ley MB, Meggouh M, Moury R, Peinecke K, Felderhoff M. Development of hydrogen storage tank systems based on complex metal hydrides. *Materials* 2015; 8:5891–921. <https://doi.org/10.3390/ma8095280>.
- [103] Bürger I, Sourmelis Terzopoulos VE, Kretschmer C, Kölbig M, Brack C, Linder M. Lightweight reactor design by additive manufacturing for preheating applications using metal hydrides. *Int J Hydrogen Energy* 2021;46:28686–99. <https://doi.org/10.1016/j.ijhydene.2021.06.091>.
- [104] Weckerle C, Bürger I, Linder M. Novel reactor design for metal hydride cooling systems. *Int J Hydrogen Energy* 2017;42:8063–74. <https://doi.org/10.1016/j.ijhydene.2017.01.066>.
- [105] Pohlmann C, Röntzsch L, Heubner F, Weißgärber T, Kieback B. Solid-state hydrogen storage in Hydrallloy-graphite composites. *J Power Sources* 2013;231: 97–105. <https://doi.org/10.1016/j.jpowsour.2012.12.044>.
- [106] Dieterich M, Pohlmann C, Bürger I, Linder M, Röntzsch L. Long-term cycle stability of metal hydride-graphite composites. *Int J Hydrogen Energy* 2015;40: 16375–82. <https://doi.org/10.1016/j.ijhydene.2015.09.013>.
- [107] Nashchekin MD, Minko MV, Morgunova SB, Minko KB. Enhancement of heat- and mass-transfer processes in a metal-hydride flow-through hydrogen-purification reactor. *Int J Hydrogen Energy* 2020;45:25013–29. <https://doi.org/10.1016/j.ijhydene.2020.06.233>.
- [108] Manickam K, Mistry P, Walker G, Grant D, Buckley CE, Humphries TD, et al. Future perspectives of thermal energy storage with metal hydrides. *Int J Hydrogen Energy* 2019;44:7738–45. <https://doi.org/10.1016/j.ijhydene.2018.12.011>.
- [109] Abdin Z, Khalilpour K, Catchpole K. Projecting the levelized cost of large scale hydrogen storage for stationary applications. *Energy Convers Manag* 2022;270: 116241. <https://doi.org/10.1016/j.enconman.2022.116241>.
- [110] Modi P, Aguey-Zinsou KF. Room temperature metal hydrides for stationary and heat storage applications: a review. *Front Energy Res* 2021;9:1–25. <https://doi.org/10.3389/fenrg.2021.616115>.
- [111] Lasher S, Stratonova M, Thijssen J. Hydrogen technical analysis. 2002.
- [112] Wang H, Liu Y, Zhang J. Hydrogen purification by Mg alloy hydrogen adsorbent. *Adsorption* 2022;28:85–95. <https://doi.org/10.1007/s10450-021-00348-2>.
- [113] Thangarasu S, Palanisamy G, Im YM, Oh TH. An alternative platform of solid-state hydrides with polymers as composite/encapsulation for hydrogen storage applications: effects in intermetallic and complex hydrides. *Int J Hydrogen Energy* 2023;48:21429–50. <https://doi.org/10.1016/j.ijhydene.2022.02.115>.
- [114] Almeida Neto GR de, Mathews FH, Gonçalves Beatrice CA, Leiva DR, Pessan LA. Fundamentals and recent advances in polymer composites with hydride-forming metals for hydrogen storage applications. *Int J Hydrogen Energy* 2022;47: 34139–64. <https://doi.org/10.1016/j.ijhydene.2022.08.004>.
- [115] Pimm AJ, Garvey SD, de Jong M. Design and testing of Energy Bags for underwater compressed air energy storage. *Energy* 2014;66:496–508. <https://doi.org/10.1016/j.energy.2013.12.010>.
- [116] Maloney P. Hydrostor comes ashore to turn old coal plants into compressed-air storage. Util Dive, <https://www.utilitydive.com/news/hydrostor-comes-ashore-to-turn-old-coal-plants-into-compressed-air-storage/441017/>. [Accessed 8 March 2024].
- [117] Pimm AJ, Garvey SD. Analysis of flexible fabric structures for large-scale subsea compressed air energy storage. *J Phys Conf Ser* 2009;181:12049. <https://doi.org/10.1088/1742-6596/181/1/012049>.
- [118] Ergenics I. Capture of liquid hydrogen boil off with metal hydride absorbers. *New Jersey: Wyckoff*; 1984.
- [119] Fiaschi D, Manfrida G, Secchi R, Tempesti D. A versatile system for offshore energy conversion including diversified storage. *Energy* 2012;48:566–76. <https://doi.org/10.1016/j.energy.2012.10.006>.
- [120] Lim SD, Mazzoleni AP, Park JK, Ro PI, Quinlan B. Conceptual design of ocean compressed air energy storage system. *Mar Technol Soc J* 2013;47:70–81. <https://doi.org/10.4031/MTSJ.47.2.5>.
- [121] William H. Experiments on the quantity of gases absorbed by water, at different temperatures, and under different pressures. *Philos Trans R Soc* 1803;(83): 29–274. <https://doi.org/10.1098/rstl.1803.0004>.
- [122] Smith B, Frame BJ, Anovitz LM, Armstrong T. Composite technology for hydrogen pipelines technical targets. *Oak Ridge*; 2008.
- [123] San Marchi C, Somerdar BP. Technical reference on hydrogen compatibility of materials - 8100 polymers. *Livermore*; 2008.
- [124] Slocum AH, Fennell GE, Dündar G, Hodder BG, Meredith JDC, Sager MA. Ocean renewable energy storage (ORES) system: analysis of an undersea energy storage concept. *Proc IEEE* 2013;101:906–24. <https://doi.org/10.1109/JPROC.2013.2242411>.
- [125] Puchta M, Bard J, Dick C, Hau D, Krautkremer B, Thalemann F, et al. Development and testing of a novel offshore pumped storage concept for storing energy at sea – Stensea. *J Energy Storage* 2017;14:271–5. <https://doi.org/10.1016/j.est.2017.06.004>.
- [126] Dick C, Puchta M, Bard J, StEnSea – results from the pilot test at Lake Constance. *J Energy Storage* 2021;42:103083. <https://doi.org/10.1016/j.est.2021.103083>.
- [127] Hahn H, Hau D, Dick C, Puchta M. Techno-economic assessment of a subsea energy storage technology for power balancing services. *Energy* 2017;133:121–7. <https://doi.org/10.1016/j.energy.2017.05.116>.
- [128] Hunt JD, Zakeri B, de Barros AG, Filho WL, Marques AD, Barbosa PSF, et al. Buoyancy Energy Storage Technology: an energy storage solution for islands, coastal regions, offshore wind power and hydrogen compression. *J Energy Storage* 2021;40:1–14. <https://doi.org/10.1016/j.est.2021.102746>.
- [129] Shiva Kumar S, Lim H. An overview of water electrolysis technologies for green hydrogen production. *Energy Rep* 2022;8:13793–813. <https://doi.org/10.1016/j.egy.2022.10.127>.
- [130] Shiva Kumar S, Himabindu V. Hydrogen production by PEM water electrolysis – a review. *Mater Sci Energy Technol* 2019;2:442–54. <https://doi.org/10.1016/j.mset.2019.03.002>.
- [131] El-Shafie M. Hydrogen production by water electrolysis technologies: a review. *Results Eng* 2023;20:101426. <https://doi.org/10.1016/j.rineng.2023.101426>.
- [132] Lototsky MV, Yartys VA, Pollet BG, Bowman RC. Metal hydride hydrogen compressors: a review. *Int J Hydrogen Energy* 2014;39:5818–51. <https://doi.org/10.1016/j.ijhydene.2014.01.158>.
- [133] Rusanov AV, Solovoy VV, Lototsky MV. Thermodynamic features of metal hydride thermal sorption compressors and perspectives of their application in hydrogen liquefaction systems. *J Phys Energy* 2020;2. <https://doi.org/10.1088/2515-7655/ab7bf4>.
- [134] Stamatakis E, Zoulias E, Tzamalidis G, Massina Z, Analytis V, Christodoulou C, et al. Metal hydride hydrogen compressors: current developments and early markets. *RENEW Energy* 2018;127:850–62. <https://doi.org/10.1016/j.renene.2018.04.073>.
- [135] IRENA. Green hydrogen cost reduction: scaling up electrolyzers to meet the 1.5°C climate goal. *International Renewable Energy Agency* 2020;65. <https://www.ire>

- na.org/-/media/Files/IRENA/Agency/Publication/2020/Dec/IRENA_Green_hydrogen_cost_2020.pdf.
- [136] Beeri O, Cohen D, Gavra Z, Johnson JR, Mintz MH. Thermodynamic characterization and statistical thermodynamics of the TiCrMn–H₂(D₂) system. *J Alloys Compd* 2000;299:217–26. [https://doi.org/10.1016/S0925-8388\(99\)00798-7](https://doi.org/10.1016/S0925-8388(99)00798-7).
- [137] Johnson T, Mallow A, Bowman R, Barton Smith D, Anovitz L, Jensen C. Metal hydride compressor for high-pressure (>875 bar) hydrogen delivery. 2022.
- [138] Guo X, Wang S, Liu X, Li Z, Lü F, Mi J, et al. Laves phase hydrogen storage alloys for super-high-pressure metal hydride hydrogen compressors. *Rare Met* 2011;30:227–31. <https://doi.org/10.1007/s12598-011-0373-7>.
- [139] Gray EMA. Alloy selection for multistage metal-hydride hydrogen compressors: a thermodynamic model. *Int J Hydrogen Energy* 2021;46:15702–15. <https://doi.org/10.1016/j.ijhydene.2021.02.025>.
- [140] Bernauer H, Schmidt-Inh T. Construction and testing of a stationary hydrogen store. Mülheim a.d. Ruhr. 1988.
- [141] Fashu S, Lototskyy M, Davids MW, Pickering L, Linkov V, Tai S, et al. A review on crucibles for induction melting of titanium alloys. *Mater Des* 2020;186:108295. <https://doi.org/10.1016/j.matdes.2019.108295>.
- [142] Friedrich B. Large-scale production and quality assurance of hydrogen storage (battery) alloys. *J Mater Eng Perform* 1994;3:37–46. <https://doi.org/10.1007/BF02654497>.
- [143] Wang R, Luo X, Zhao C, Sun M, Li N. Experimental study on the corrosion of AlN refractories used as crucibles for induction melting of TiNi alloys. *J Mater Res Technol* 2024;30:4920–8. <https://doi.org/10.1016/j.jmrt.2024.04.228>.
- [144] Nayebossadri S, Book D. Development of a high-pressure Ti-Mn based hydrogen storage alloy for hydrogen compression. *Renew Energy* 2019;143:1010–21. <https://doi.org/10.1016/j.renene.2019.05.052>.
- [145] Cao Z, Ouyang L, Wang H, Liu J, Sun D, Zhang Q, et al. Advanced high-pressure metal hydride fabricated via Ti–Cr–Mn alloys for hybrid tank. *Int J Hydrogen Energy* 2015;40:2717–28. <https://doi.org/10.1016/j.ijhydene.2014.12.093>.
- [146] Cao Z, Zhou P, Xiao X, Zhan L, Jiang Z, Piao M, et al. Studies on Ti-Zr-Cr-Mn-Fe-V based alloys for hydrogen compression under mild thermal conditions of water bath. *J Alloys Compd* 2021;892:162145. <https://doi.org/10.1016/j.jallcom.2021.162145>.
- [147] Zhou P, Cao Z, Xiao X, Zhan L, Li S, Li Z, et al. Development of Ti-Zr-Mn-Cr-V based alloys for high-density hydrogen storage. *J Alloys Compd* 2021;875:160035. <https://doi.org/10.1016/j.jallcom.2021.160035>.
- [148] Puzkiel J, Bellosta von Colbe JM, Jepsen J, Mitrokhin SV, Movlaev E, Verbetsky V, et al. Designing an AB₂-type alloy (TiZr-CrMnMo) for the hybrid hydrogen storage concept. *Energies* 2020;13. <https://doi.org/10.3390/en13112751>.
- [149] Proctor CL. Internal combustion engines. In: Third E, editor. Meyers RABT-E of PS and T. *Encycl. Phys. Sci. Technol.* third ed. New York: Academic Press; 2003. p. 33–44. <https://doi.org/10.1016/B0-12-227410-5/00350-1>.
- [150] Yahya SM. Turbines compressors and fans. Tata McGraw-Hill; 2005.
- [151] Johansson J, Lerines J, Walton K, Yilmaz E, Zindel E. Hydrogen power and heat with Siemens Energy gas turbines. Erlangen: Siemens Energy Global GmbH & Co. KG; 2022.
- [152] Eroglu A, Larfeldt J, Klapdor EV, Yilmaz E, Prasad VN, Prade B, et al. Hydrogen capabilities of siemens energy gas turbines, an oem perspective. In: Gas turbines a carbon-neutral soc. 10th int. Gas turbine conf.; 2021. p. 1–12.
- [153] Sanz W, Braun M, Jerichar H, Platzer M. Adapting the zero-emission Graz cycle for hydrogen combustion and investigation of its Part Load behaviour. In: Proc. ASME turbo expo 2016 turbomach. Tech. Seoul: Conf. Expo; 2016. p. 1–10.
- [154] Shiozaki S, Fujii T, Takenaga K, Ozawa M, Yamada A. 6 - gas turbine combined cycle. In: Ozawa M, Asano HBT-A, editors. PB, editors. JSME ser. Therm. Nucl. Power gener., vol. 2. Elsevier; 2021. p. 305–44. <https://doi.org/10.1016/B978-0-12-820360-6.00006-0>.
- [155] Guénan T Le, Gravaud I. Risk assessment of reversible storage of O₂ and CO₂ in salt caverns for large-scale energy storage. *Environmental Science, Engineering* 2018.
- [156] Society TR. Large-scale electricity storage - supplementary information. 2023.